BMC Biology

RESEARCH

Open Access

LADS: a powerful vaccine platform for cancer immunotherapy and prevention

Jing Sun[1†], Jing Wang[1†], Xin Jiang[1†], Jing Xia[1], Yue Han[1], Mianmian Chen[1], Jiali Xu[1], Simin Deng[1], Changyong Cheng[1*] and Houhui Song[1*]

Abstract

Background The intracellular bacterium *Listeria monocytogenes* is an attractive vector for cancer immunotherapy as it can effectively deliver tumor antigens to antigen-presenting cells, leading to a robust antitumor response.

Results In this study, we developed a novel vaccine platform called *Listeria*-based Live Attenuated Double Substitution (LADS), which involves introducing two amino acid substitutions (N478AV479A) into the virulence factor listeriolysin O (LLO). LADS is a safe vaccine platform, with an attenuation of nearly 7000-fold, while retaining complete immunogenicity due to the absence of deletion of any virulence factors. We developed two LADS-based vaccines, LADS-E7 and LADS-AH1, which deliver the human papillomavirus (HPV) type 16 E7 oncoprotein and murine colon carcinoma immunodominant antigen AH1, respectively. Treatment with LADS-E7 or LADS-AH1 significantly inhibited and regressed established tumors, while also dramatically increasing the populations of tumor-infiltrated antigen-specific $CD8^+$ T cells. RNA-sequencing analysis of tumor tissue samples revealed that LADS-E7 altered the expression of genes related to the immune response. Moreover, intratumoral injection of LADS-based vaccines induced strong antitumor responses, generating systemic antitumor responses to control distant tumor growth. Encouragingly, LADS-E7 or LADS-AH1 immunization effectively prevented tumor formation and growth.

Conclusions Our findings demonstrate that LADS-based vaccines represent a more powerful platform for the development of immunotherapeutic and preventive vaccines against cancers and infectious diseases.

Keywords Aattenuated *Listeria monocytogenes*, LADS, Tumor immunotherapy, Tumor prevention, Listeriolysin O, Tumor-associated antigen

Background

Listeria monocytogenes (LM) is an intracellular foodborne pathogen that can proliferate in a variety of cells, including epithelial cells, fibroblasts, and macrophages [1]. Once the bacterium successfully invades into host cells, it maintains the ability to activate the adaptive immune response via the major histocompatibility complex (MHC) pathways [2]. Those bacteria that do not escape the host cell phagosome elicit an immune response through the MHC II pathway with subsequent activation of $CD4^+$ T cells. However, LM has evolved many sophisticated mechanisms to escape into the cytosols of infected cells mediated by many virulence factors. Listeriolysin O (LLO), a pore-forming cytolysin,

†Jing Sun, Jing Wang and Xin Jiang contributed to this work equally.

*Correspondence:
Changyong Cheng
lamge@zafu.edu.cn
Houhui Song
songhh@zafu.edu.cn
[1] Key Laboratory of Applied Biotechnology on Animal Science & Veterinary Medicine of Zhejiang Province, Zhejiang Engineering Research Center for Veterinary Diagnostics & Advanced Technology, Zhejiang International Science and Technology Cooperation Base for Veterinary Medicine and Health Management, Belt and Road International Joint Laboratory for One Health and Food Safety, China-Australia Joint Laboratory for Animal Health Big Data Analytics, College of Veterinary Medicine, Zhejiang A&F University, 666 Wusu Street, Lin'an District, Hangzhou, Zhejiang Province 311300, China

enables *Listeria* to perforate the membranes of phagocytic cells such as macrophages and dendritic cells, after which it escapes from cytoplasmic vacuoles and enters the cytoplasm, thereby spreading to the neighboring cells. Once outside the phagosome, peptides secreted by the bacterium enter the host cell cytosol where they can be degraded by proteasomes and loaded onto MHC I molecules for presentation to $CD8^+$ T cells for robust induction of LM-specific cytotoxic T lymphocytes (CTL) responses that protect against a subsequent exposure [3, 4]. Moreover, LM can also induce a decrease in regulatory T cells (Tregs) in tumor tissues, thereby promoting an immune response to kill tumor cells directly [5–7]. Therefore, the capacity to efficiently deliver tumor-associated antigens (TAA) to antigen-presenting cells and activate robust antitumor cellular immune responses makes LM a powerful vaccine vector for tumor immunotherapy [2, 8–10].

So far, *Listeria*-based vaccines have been widely developed for numerous malignancies that demonstrate promising efficacy in preclinical models of cancer with several candidates in various stages of clinical development [2, 3, 8, 11–17]. However, LM is a pathogenic microorganism that can cause severe listeriosis in humans with a high mortality rate, attenuation of its virulence is necessary for safety considerations as an antitumor vaccine. Early studies have employed strains containing deletions of genes involved in bacterial virulence to accomplish reliable attenuations of LM-based vaccine strains. While infection with the virulent LM strains can lead to the formation of robust memory T cell responses, several studies have found that attenuated strains result in improved immune memory and protective responses [18, 19]. To date, the most widely employed strategy to attenuate LM involves lacking the transcriptional regulator PrfA [17], or the other two virulence factors, ActA and InlB [18, 20]. The resultant strain Δ*actA*/Δ*inlB* has been best known as the Live Attenuated Double-Deleted (LADD) platform (Aduro BioTech Inc.) that forms the basis for several vaccines in clinical trials. Besides, an alternative attenuation strategy has been developed using the Δ*dal*/Δ*dat* strain (Lmdd) from which the *dal* and *dat* genes required to synthesize D-alanine to build peptidoglycan and lipoteichoic have been deleted [21–23]. However, these virulence factors (such as PrfA, LLO, and ActA) are known to play important roles for the LM escaping into the cytosol and promoting the delivery of TAA to the proteasome, which can enhance the efficiency of antigen processing and MHC class I presentation [24–27]. Additionally, these virulence factors have adjuvant properties to activate Toll-like receptor 4 (TLR4) signaling pathway, inducing the production of inflammatory cytokines such as interleukin (IL)−6, IL-12, IL-18, and interferon (IFN)-γ, promoting the differentiation of activated $CD4^+$ T cells into Type 1 helper (Th1) cells [28–30]. It is very likely that the current attenuated LM platform displays reduced immunogenicity and affects the priming of cellular anti-tumor immune response owing to the deletion of the virulence factors. Therefore, a new attenuated LM vaccine platform that retains high immunogenicity need to be constructed.

In the present study, we developed a novel live-attenuated LM immunotherapy platform (Live Attenuated Double Substitution, LADS) in which none of the genes was deleted but only introduced a substitution of two residues in the carboxyl-terminal of LLO (N478AV479A). LADS can be rapidly cleared in mice without significant organ damage following intravenous administration and is approximately 7000-fold attenuated relative to the wild-type LM. More importantly, LADS secretes a detoxified LLO ($LLO_{N478AV479A}$) and can generate all bacterial antigens (such as ActA) as the wild-type strain, display high immunogenicity and have been demonstrated to act as adjuvants to boost therapeutic immune responses against tumors [17, 25, 27]. Based on this novel platform, two genetically modified vaccines (LADS-E7 and LADS-AH1) that secrete the human papillomavirus (HPV) type 16 antigen E7 and the murine colon carcinoma antigen AH1, respectively, with a fusion to LLO, were developed and tested for their antitumor effects in established murine tumor models. Cervical cancer is the fourth most common cancer in women worldwide and is almost exclusively caused by HPV infection, with most cases being attributed to HPV subtypes 16 and 18 [31–34]. HPV expresses the E6 and E7 oncoproteins that directly promote cell division and tumorigenesis, and E7 is necessary to maintain the malignant state of the tumor cells, thereby serving as a target for immunotherapy [35, 36]. AH1 is an antigenic peptide presented on $H\text{-}2L^d$, first identified as the immunodominant antigen of the murine colon carcinoma cell line CT26 [37]. It derives from the endogenous murine leukemia virus envelope glycoprotein 70 (gp70), and it is highly expressed in a multitude of murine tumor cell lines of different histological origins, while being virtually undetectable in healthy murine organs [38, 39]. Encouragingly, we demonstrate that the novel LADS-based cancer vaccines, LADS-E7 and LADS-AH1, are safe and can trigger strong cellular immune responses, particularly the tumor antigen-specific $CD8^+$ cytotoxic T cells in the infiltrated tumors, to mediate robust tumor suppression and clearance in the murine cervical cancer and colon carcinoma models. RNA-sequencing analysis showed that a large number of genes affected by vaccination of LADS-E7 were enriched in immune response. Moreover, intratumoral injection of the LADS-based vaccines also induced

strong antitumor responses and can generate systemic antitumor responses to control distant tumor growth. Surprisingly, the immunization of LADS-E7 or LADS-AH1 achieved terrific effects on preventing tumor formation and growth. Therefore, the impressive antitumor and prevention efficacy of LADS-based vaccines makes LADS a new and attractive delivering platform to further develop more promising tumor vaccines for clinical cancer immunotherapy and prevention.

Results

LADS secreting $LLO_{N478AV479A}$ with decreased hemolytic activity is unable to grow intracellularly in macrophages

As we have previously established that the residues Asn478 and Val479 are new active sites that are required for LLO hemolytic activity [40], the substitution mutation (N478AV479A) was introduced into the chromosome on the background of the wild-type LM EGD-e, resulting in the mutant strain LADS (Additional file 1: Fig. S1A). As shown by immunoblotting, LADS could express and secrete $LLO_{N478AV479A}$ in comparable amounts to wild-type LLO, demonstrating that these residue substitutions did not affect LLO synthesis and secretion (Additional file 1: Fig. S1B, C). Moreover, the mutations had no significant influence on this bacterium's in vitro growth (Additional file 1: Fig. S1D). However, the hemolytic ability recorded in the supernatants of LADS was dramatically impaired relative to the wild-type strain (Additional file 1: Fig. S1E), with the supernatant of centrifuged blood appearing much lighter in red compared to the WT group, which is entirely consistent with our previous findings that the novel residues N478 and V479 are crucial for LLO-mediated pore-forming and hemolytic activity. To investigate the ability of LADS to grow intracellularly, the murine-derived macrophage cell lines (J774A.1 and RAW264.7) and the primary bone marrow-derived macrophages (BMDMs) were used as the infection models. As indicated in Additional file 1: Fig. S1F-H, LADS was unable to grow intracellularly within all the three macrophage types, similar to the circumstance for the Δ*hly* mutant strain where LLO has been deleted, and bacteria failed to escape from vacuolar during intracellular infection (Additional file 1: Fig. S1F, G, and H). These data collectively indicated that LADS is completely unable to grow intracellularly in macrophages.

LADS is highly attenuated and safe for potential use as a live vaccine vector

LM is responsible for foodborne listeriosis and can cause severe symptoms for humans [41, 42]. Therefore, it is essential to guarantee the safety of LADS for potential use as a vaccine vector. The virulence of LADS was evaluated in a murine listeriosis model in terms of median lethal dose (LD50) values and bacterial loading and clearance in mouse livers and spleens. For LD50 value determination, the ICR mice were inoculated intraperitoneally with various bacterial concentrations, and their survival was monitored until no mice died. Encouragingly, the LD50 value for LADS and LADS-E7 is $10^{9.07}$ and $10^{9.68}$ CFU, respectively (Additional file 2:Fig. S2A, D), extremely higher than the wild-type EGD-e with the LD50 of $10^{5.25}$ CFU (Additional file 2: Fig. S2B) and even higher than the avirulent strain Δ*hly* with the LD50 value of $10^{8.74}$ CFU (Additional file 2:Fig. S2C), indicating that the virulence of LADS and LADS-E7 are attenuated nearly 7000-fold relative to its parent strain. Additionally, the LD50 value for LADD-E7, which is constructed based on a current widely used live-attenuated LM vaccine platform (LADD), is $10^{8.64}$ CFU and lower than that of LADS-E7 (Additional file 2: Fig. S2E), indicating that the LADS-based vaccine is safer than that of LADD. Moreover, no detectable LADS bacteria were recovered from the mouse livers and spleens after inoculated intraperitoneally with 10^6 CFUs bacteria for 24 or 48 h. In contrast, about $10^4 \sim 10^8$ CFUs bacteria could be detected for the wild-type strain recovered from the mouse organs (Additional file 2: Fig. S2F and G). Next, we further investigated the kinetics of bacterial clearance in the organs from C57BL/6 J mice infected intravenously via caudal vein with a high dose of 1.9×10^8 CFUs LADS, which we expected to provide a biosafety basis for the following tumor therapy experiments. As indicated, the amount of bacteria in target organs decreased gradually 2 days post-infection, and finally, the mice completely cleared the infection by day 6 (Additional file 2: Fig. S2H). No deaths of mice and no organ damage were observed during the whole kinetics of bacterial clearance, confirming that the novel LADS platform is safe and reliable as a vaccine vector for antitumor immunotherapy.

Vaccination with LADS confers protective immunity

The two requirements for a live vaccine platform are safety and efficacy. In Additional file 2: Fig. S2, we showed that LADS is highly attenuated and thus satisfies the safety requirement. To test the efficacy of LADS as a live vaccine, a protection study from the virulent wild-type LM infection was carried out both on ICR and C57BL/6 J mice models according to the indicated strategies. In strategy 1 (Fig. 1A), ICR mice were vaccinated intraperitoneally with 10^8 LADS on days 0 and 14. One week post the last vaccination, the mice were challenged with a lethal dose of WT LM (10^5, 10^6, or 10^7 CFUs). Two days post-challenge, the bacterial burdens from mice livers and spleens were enumerated. Vaccination with LADS provided 6-logs of protection from LM infection as no bacteria recovered from the vaccinated

mice which were challenged with a high dose of 10^6 CFUs (Fig. 1B and C). It should be noted that, based on our preliminary research, the dose of 10^7 CFU significantly exceeds the LD50 of the wild-type strain. Therefore, in our experiment, all mice inoculated with this high dose did not survive beyond 48 h, resulting in a lack of data under this specific condition. Meanwhile, we further monitored the survival kinetics of these vaccinated mice which were challenged with various doses of WT bacteria for a duration of 8 days. The data showed that vaccination with LADS provided a complete 7-logs of protection as all the vaccinated mice survived, while all the mice vaccinated with Hanks' Balanced Salt Solution (HBSS, control) died before day 7 even challenged with a low 10^5 dose of WT bacteria (Fig. 1D, E, F). In strategy 2 (Fig. 1G), C57BL/6 J mice were vaccinated with either 10^5 or 10^6 CFUs LADS via tail vein, and the mice were challenged with 10^5 WT bacteria via the same routine 2 weeks-post vaccination. Three days post-challenge, CFU from the mice organs were enumerated, showing that vaccination with either 10^5 or 10^6 CFUs LADS provided significant protection from intravenous bacterial infection (Fig. 1H). The survival kinetics indicated that vaccination with 10^6 CFUs LADS conferred 100% protection and 10^5 CFUs LADS with 80% protection (Fig. 1I). Collectively, LADS is a highly attenuated LM strain capable of inducing robust protective immunity, which further makes LADS a safe and reliable vaccine platform for antitumor immunotherapy.

LADS-based vaccines specifically secrete the $LLO_{N478AV479A}$-fused antigens

Based on the attenuated LADS platform, we constructed two LADS-based vaccine strains that express E7 antigen (LADS-E7), or AH1 antigen (LADS-AH1) fused to the residual-hemolytic $LLO_{N478AV479A}$ via the homologous recombination strategy as described in Additional file 3: Fig. S3A. AH1 is a dominant H-2Ld-restricted $CD8^+$ T cell epitope derived from endogenous retroviral antigen gp70 [37], and E7 is the HPV type 16-derived oncoprotein [43]. Expression and secretion of the $LLO_{N478AV479A}$-E7 or $LLO_{N478AV479A}$-AH1 fusion proteins from LADS-E7 or LADS-AH1 were detected in the cell culture supernatants and whole bacterial proteins after in vitro growth of the bacteria. As indicated, LADS-E7 synthesized and secreted the fusion protein $LLO_{N478AV479A}$-E7 as detected with both anti-LLO and anti-E7 antibodies (Additional file 3: Fig. S3B). Since the anti-AH1 antibodies were not available from the supplier, we detected the fusion protein $LLO_{N478AV479A}$-AH1 with anti-LLO antibodies only. Likewise, LADS-AH1 was also capable of producing the fusion protein $LLO_{N478AV479A}$-AH1 as displayed in Additional file 3: Fig. S3C. As expected, the vaccine strains LADS-E7 and LADS-AH1 exhibited a comparable in vitro growth kinetics to LADS (Additional file 3: Fig. S3D), suggesting that introducing foreign antigens had no impact on the growth characteristics of LADS. Moreover, the hemolytic activities of fused $LLO_{N478AV479A}$-E7 or AH1 secreted by LADS-E7 or LADS-AH1 were remarkably impaired due to the identified mutations present on the residues N478V479 that have previously been found required for LLO pore-forming activity (Additional file 3: Fig. S3E). Taken together, the LADS-based vaccines LADS-E7 and LADS-AH1 were successfully constructed that were capable of efficiently secreting the LLO-fused antigens.

LADS-Ag vaccination efficiently regresses tumors growth in mice

To evaluate the antitumor efficacy of the LADS-E7 vaccine, C57BL/6 J mice were subcutaneously implanted with the HPV16-derived E7 expressing TC-1 tumor cells, which has been working as a surrogate for human HPV16 tumors [43]. After tumors had reached a palpable size of about 5 mm, C57BL/6 J mice bearing TC-1 tumors were treated twice via tail vein immunization with LADS-E7, LADS, or HBSS buffer 1-week intervals according to the strategy as described (Fig. 2A). Excitingly, Fig. 2B illustrates that the tumor volumes and growth rates in mice administered LADS-E7 had an average of 24.96 mm^3, which is significantly reduced compared to the LADS group, averaging 1165.23 mm^3, and the HBSS group,

(See figure on next page.)

Fig. 1 Vaccination with LADS confers protective immunity in mice. **A** The strategy for the immune protective assay in ICR mice. Mice were vaccinated intraperitoneally with HBSS or 10^8 LADS on days 0 and 14. One week post the last vaccination, the mice were challenged intraperitoneally with a lethal dose of WT LM (10^5, 10^6, or 10^7 CFUs). **B,C** The proliferation of WT bacteria from the mice after vaccination of LADS. Two days post-challenge, bacterial CFUs were enumerated from the mice livers (**B**) and spleens (**C**). Data are expressed as mean ± SEM of the $\log_{10}$CFU per organ for each group. **D–F** The Kaplan–Meier survival curves of mice infected with 10^5 (**D**), 10^6 (**E**), or 10^7 (**F**) WT LM after vaccination of LADS. **G** The strategy for the immune protective assay in C57BL/6 J mice. Mice were vaccinated intravenously with 10^5 or 10^6 LADS on day 0. Two weeks post vaccination, the mice were challenged with 10^5 WT bacteria via tail vein. **H** The proliferation of WT bacteria from the mice after vaccination of LADS. Three days post-challenge, bacterial CFUs were enumerated from the mice livers and spleens. Data are expressed as mean ± SEM of the $\log_{10}$CFU per organ for each group. **I** The Kaplan–Meier survival curves of mice infected with WT LM after vaccination of 10^5 or $10.^6$ LADS. Data (**B** and **C**) are expressed as mean ± SEM of three replicates. *$p < 0.05$, **$p < 0.01$, and ***$p < 0.001$

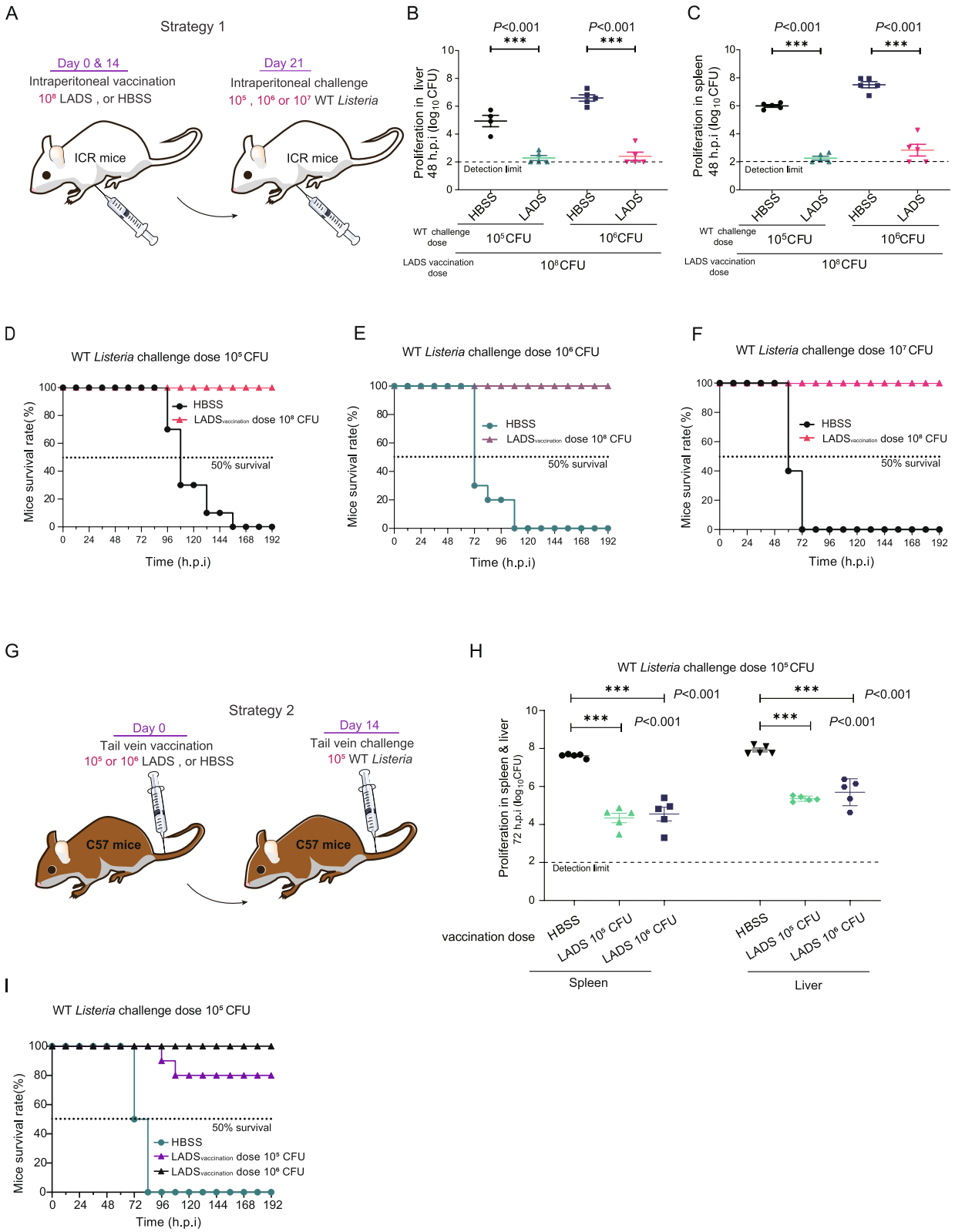

Fig. 1 (See legend on previous page.)

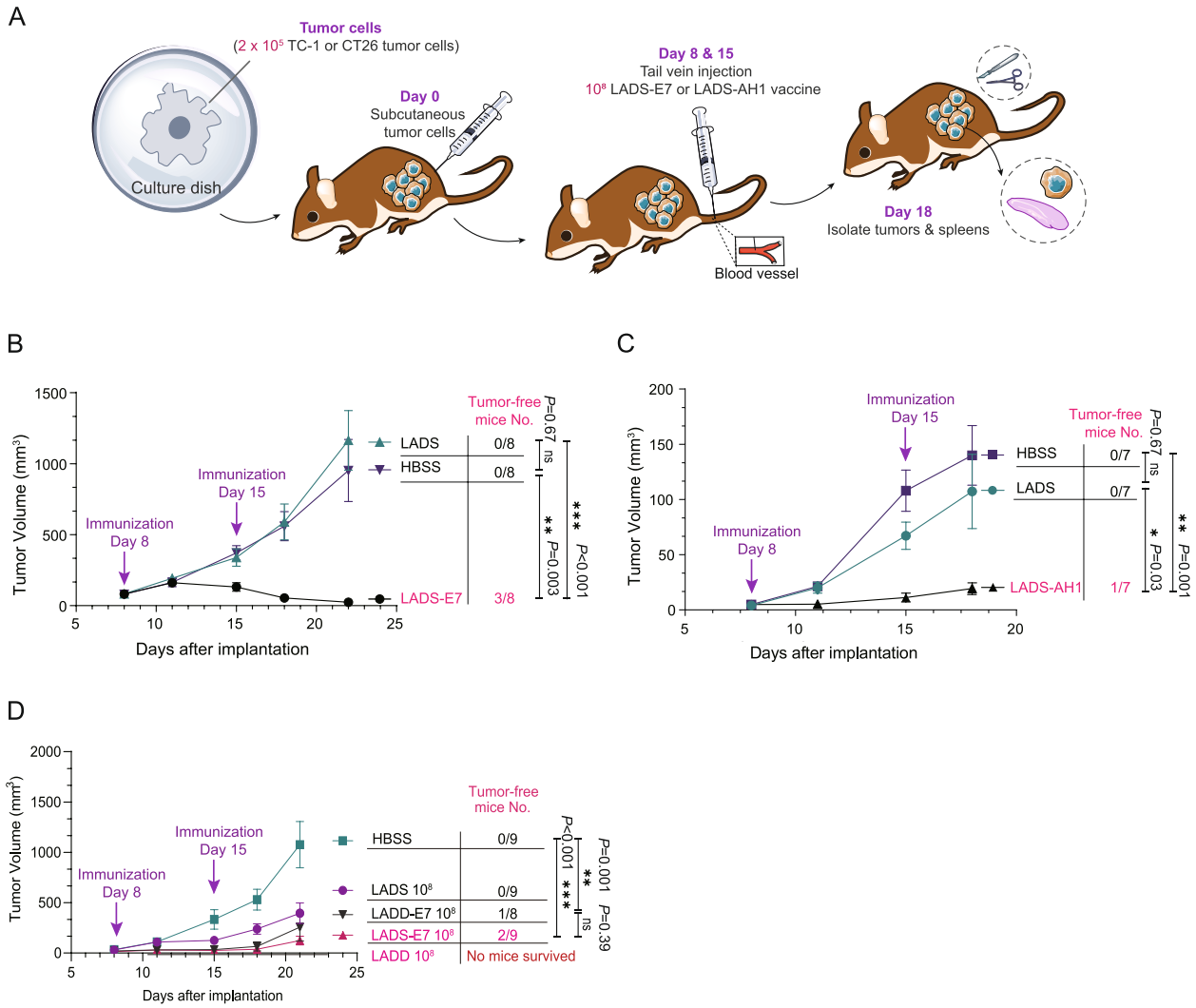

Fig. 2 Vaccination of LADS-Ag causes regression of established tumors. **A** Schedule of immunotherapy procedures in the tumor-bearing models. C57BL/6 J or BALB/c mice were subcutaneously injected with 2×10^5 TC-1 or CT26 tumor cells, and after the tumor reached a size of 4–5 mm in diameter, tumor-bearing mice were intravenously administered with LADS-E7 or LADS-AH1 on days 8 and 15. Tumors and spleens were then harvested for further analysis on day 18. **B** The growth of TC-1 tumors in mice vaccinated with LADS-E7 was monitored at the indicated time points. **C** The growth of CT26 tumors in mice vaccinated with LADS-AH1 was monitored at the indicated time points. **D** Growth curve of TC-1 tumors in mice vaccinated with LADD-E7 or LADS-E7 at the indicated time points. Tumor volume was expressed as mean ± SEM of eight mice in each group. The numbers of tumor-free mice are indicated in the figures. *$p < 0.05$, **$p < 0.01$, and ***$p < 0.001$

averaging 951.98 mm^3. More importantly, the administration of LADS-E7 also led to a complete regression of established tumors in three of eight mice (Fig. 2B). By contrast, no reduction in tumor growth was observed in mice treated with LADS or HBSS at any time point, and all the mice in these two groups were humanely sacrificed when the tumor reached 20 mm (Fig. 2B). To test whether this striking antitumor response could be observed in distinct genetic mice backgrounds. The BALB/c mice were employed as the tumor-bearing model. AH1 antigen is expressed in CT26 tumor cells [44], which allowed us to test the efficacy of the LADS-AH1 vaccine in BALB/c mice bearing this tumor. The CT26 tumor-bearing mice were treated with LADS-AH1 or LADS using the same immunotherapy strategy as LADS-E7. As anticipated, immunization with LADS-AH1 elicited a robust antitumor response. The tumor volumes and growth kinetics in the LADS-AH1 treated mice, with an average volume of 23.08 mm^3, demonstrated a remarkable regression compared to the control groups. Specifically, the LADS group exhibited an average tumor volume of 107.34 mm^3, while the HBSS group had an even higher average of 139.91

mm^3 (Fig. 2C). Additionally, the differences in therapeutic efficacy between LADD-E7 and LADS-E7 were evaluated according to the strategy as described in Fig. 2A. After immunization with 10^8 CFU LM based vaccine, one mouse died in LADD-E7-injected group whereas all mice survive in LADS-E7 group, this might be due to the higher virulence of LADD-E7 as we show in Additional file 2: Fig. S2D and Additional file 2: Fig. S2E. The size of tumor in LADD-E7-injected group trend to be bigger than that in LADS-E7 group 21 days after tumor implantation, and the proportion of tumor-free mouse in LADD-E7-treated group lower than that of LADS-E7 group (Fig. 2D). These data demonstrate that LADS-based vaccines exerted strong antitumor effects in the established tumor models, and this LADS-induced antitumor efficacy requires expression of a relevant tumor antigen delivered by LADS, thereby providing a new potential strategy for cancer immunotherapy.

Vaccination of LADS-Ag induces robust Ag-specific $CD8^+$ T cells in tumors

Cancer development is highly influenced by the tumor microenvironment (TME), underlying the importance of TME components in tumor immunotherapy. Tumor-specific $CD8^+$ cytotoxic T cells are the primary type of lymphocytes in cell-mediated immunity and play a central role in inducing efficient immune responses against tumors [45, 46]. To elucidate whether vaccination with LADS-Ag induced Ag-specific CTLs can infiltrate the tumors, the populations of tumor antigen Ag-specific $CD8^+$ T cells (stained with the H-$2D^b$ E7 and H-$2L^d$ AH1 tetramers for E7- and AH1-specific $CD8^+$ T cells, respectively) isolated from the tumor-bearing mice spleens and tumors were measured. Strikingly, the flow cytometry analysis 3 days after the last immunization with LADS-E7 showed significantly increased percentages of the E7-specific $CD8^+$ T cell frequency from splenocytes (Fig. 3A, B), compared with those from the LADS (Fig. 3C) or HBSS group (Fig. 3D). TME is the natural environment for $CD8^+$ cytotoxic T cell-mediated tumor killing. We pay more attention to the antigen-specific $CD8^+$ T cell frequency in TME than in the splenocytes. As expected, LADS-E7 treatment dramatically increased the frequency of E7-specific $CD8^+$ T cells in infiltrated tumors (Fig. 3E, F), with approximately 91 times higher than LADS or HBSS where almost no detectable E7-specific $CD8^+$ T cells were detected (Fig. 3G, H). As for LADS-AH1, immunization with this vaccine also induced a 25-fold high frequency of AH1-specific $CD8^+$ T cells in infiltrated tumors (Fig. 3I, J) compared with those from LADS (Fig. 3K) or HBSS (Fig. 3L) group where the antigen-specific $CD8^+$ T cells were in the background levels. Notably, the TME is highly immunosuppressive partially due to the fact that Tregs can suppress antitumor immunity and hamper effective antitumor immune responses [47, 48]. We next characterized Tregs populations in the mice-bearing tumors after treatments, and the data indicated that LADS-E7 treatment decreased tumor-infiltrating Treg frequency compared with the treatment of LADS or HBSS (Fig. 3M). The gating strategy for flow cytometry is shown as depicted in Additional file 4: Fig. S4A. These data collectively illustrate that LADS-E7 immunization can trigger a robust population of tumor-infiltrating antigen-specific $CD8^+$ cytotoxic T cells and induce modulation effects on the tumor microenvironment, thereby facilitating antitumor cellular immune response responses in an established tumor model.

Intratumoral injection of LADS-E7 generated systemic antitumor responses in established tumors

To investigate a potential antitumor effect of different administration routes of LADS-based vaccines, we chose LADS-E7 (with comparatively better tumor-eradicating effects) to determine whether the route of this vaccine impacts the generation of antitumor effects. C57BL/6 J mice were first implanted with 2×10^5 TC-1 tumor cells subcutaneously on both sides of the mouse abdomen according to the previous study with minor modifications [49]. Once the tumor was established, mice received an intratumoral injection of LADS-E7 on only one side on days 7, 12, and 17 (Fig. 4A). To monitor the antitumor responses, tumors on both the ipsilateral and

(See figure on next page.)

Fig. 3 LADS-Ag induces robust Ag-specific $CD8^+$ T cells in infiltrated tumors. **A** Frequency of E7 $tetramer^+$ $CD8^+$ T cells from spleens. **B–D** Representative staining of E7 tetramer and $CD8^+$ T cells from spleens. The tumor-bearing C57BL/6 J mice were immunized *i.v.* on days 8 and 15 after tumor challenge with 0.1 LD50 of LADS-E7 (**B**), LADS (**C**), or HBSS (**D**). On day 18, spleens were harvested and splenocytes stained with an H-$2D^b$ E7 tetramer and anti-CD8. **E** Frequency of E7 $tetramer^+$ $CD8^+$ T cells from tumors. **F–H** Mice were immunized as described above (**F** LADS-E7, **G** LADS, **H** HBSS), and tumors were harvested on day 18 and single-cell suspensions stained with an H-$2D^b$ E7 tetramer, anti-CD8, and anti-CD3. **I** Frequency of AH1 tetramer $CD8^+$ T cells from tumors. **J–L** Representative staining of AH1 tetramer and $CD8^+$ T cells from tumors. The tumor-bearing BALB/c mice were immunized *i.v.* on days 8 and 15 after tumor challenge with 0.1 LD50 of LADS-AH1 (**J**), LADS (**K**), or HBSS (**L**). On day 18, spleens were harvested and splenocytes stained with an H-$2L^d$ AH1 tetramer and anti-CD8. **M** Frequency of Treg in $CD4^+$ T cell population from tumors. As described above, mice were immunized with LADS-E7. Tregs were defined as $CD4^+CD25^+Foxp3.^+$ cells. Data (**A**, **E**, **I**, and **M**) are expressed as mean ± SEM of three replicates. *$p < 0.05$, **$p < 0.01$, and ***$p < 0.001$

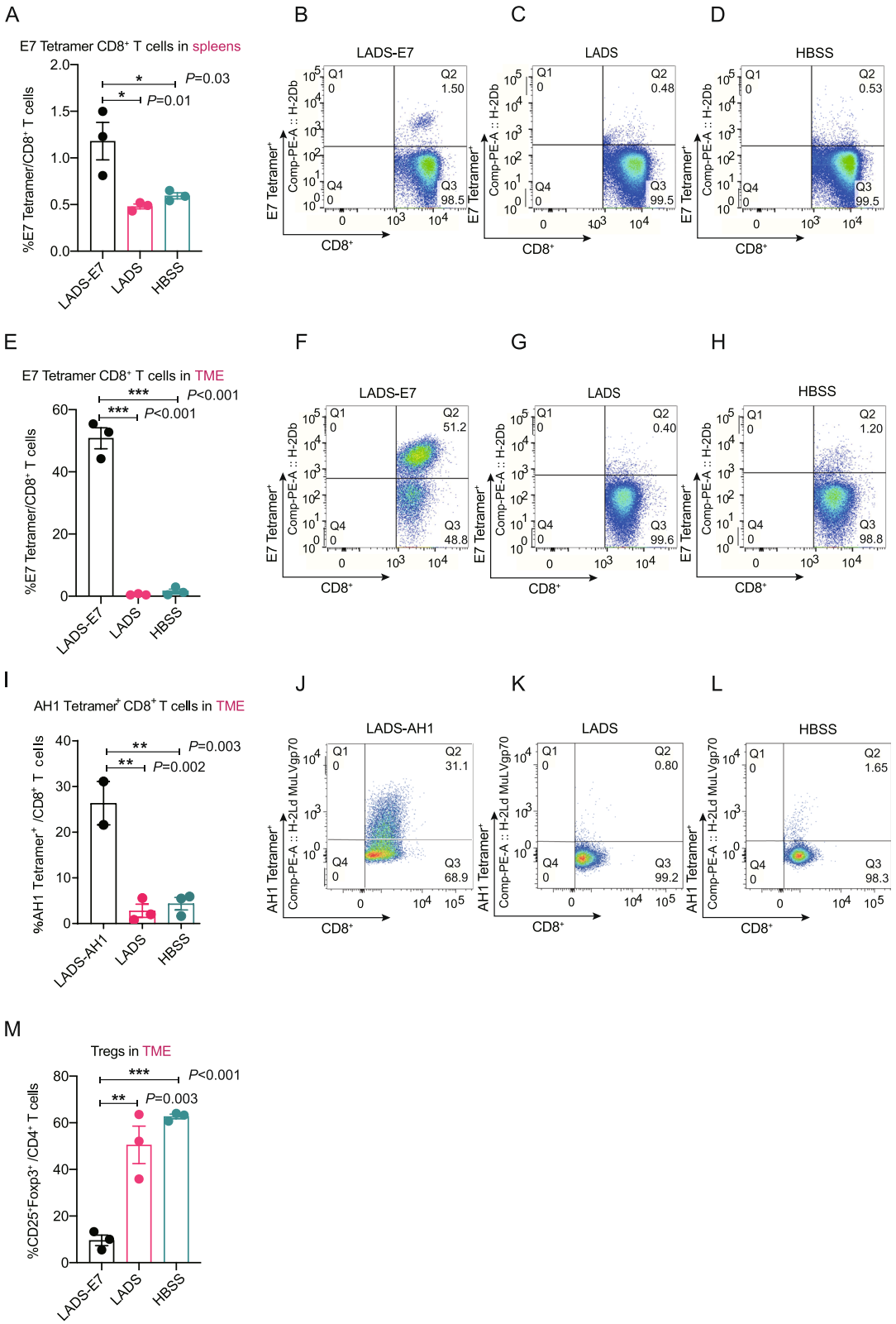

Fig. 3 (See legend on previous page.)

contralateral sides were measured twice a week. Encouragingly, we found that robust tumor regression in the LADS-E7 group was observed on both the ipsilateral and contralateral tumors compared to those vaccinated with either LADS or HBSS (Fig. 4B and C). Surprisingly, the contralateral LADS-E7 group also demonstrated therapeutic effects against the tumor. Furthermore, the proportion of tumor-associated antigen specific T cells in the TME were analyzed by flow cytometry. Immunization of LADS-E7 significantly increased the frequency of E7-specific $CD8^+$ T in both the ipsilateral (Fig. 4D and F) and contralateral (Fig. 4D and G) tumor tissues compared with those from LADS (Fig. 4D, H, and I) and HBSS (Fig. 4E) injected group. These data showed that intratumoral injection of LADS-based vaccine can potentially elicit therapeutic antitumor immunity not only in the injected tumor site but also in distant noninjected tumor lesions, termed an abscopal effect. Taken together, these results suggest that intratumoral vaccination of LADS-based vaccines can generate systemic antitumor responses to control distant tumor growth.

Vaccination of LADS-Ag confers effective prevention of tumor implantation

Our data have demonstrated that LADS-based vaccines (LADS-E7 and LADS-AH1) exert strong antitumor effects in the established TC-1 and CT26 tumor models via intravenous or intratumoral injection. Although attenuated LM has been an attractive platform for developing cancer immunotherapy vaccines, research on the feasibility of this bacterium using as a preventive cancer vaccine is very rare. Thus, to investigate whether immunization of LADS-based vaccines could provide effective tumor prevention, we implanted tumor cells into mice after immunizations of LADS-Ag, and then tumor growth was monitored (Fig. 5A). C57BL/6 J mice were immunized with LADS-E7 on days 0 and 14, and the vaccinated mice were then implanted with 2×10^5 TC-1 tumor cells on day 19. Most excitingly, the data revealed that vaccination with LADS-E7, resulting in an average tumor volume of just 1.15 mm^3, nearly achieved complete inhibition of tumor growth. Remarkably, all eight mice in this group were virtually tumor-free by the conclusion of the experiment (Fig. 5B). In stark contrast, mice vaccinated with either LADS, which had an average tumor volume of 884.72 mm^3, or HBSS, with an average of 536.16 mm^3, exhibited significant and sustained tumor growth throughout the duration of the study, as depicted in Fig. 5B. In the CT26 model, BALB/c mice were immunized with LADS-AH1 on days 0 and 14, and the vaccinated mice were then implanted with 3×10^5 CT26 tumor cells on day 19. As anticipated, vaccination with LADS-AH1 demonstrated significant tumor growth inhibition, with an average tumor volume of 106.84 mm^3. By the end of the experiment, depicted in Fig. 5C, approximately half of the mice had achieved a near-tumor-free state, showcasing the efficacy of the LADS-AH1 treatment. The efficacy for tumor prevention between LADD-E7 and LADS-E7 was measured according to the strategy in Fig. 5A. As the LADD-E7 retain the virulence in some extent and the immunization of this vaccine with 10^8 CFU can lead to the death of mice, 10^7 CFU of LADD-E7 was used for immunization. Surprisingly, all tumor cells were eliminated in LADS-E7 immunized mice 22 days after tumor implantation, whereas only a quarter of the mice completely repress the growth of tumor cells in LADD-E7-injected group (Fig. 5D). Therefore, these results demonstrated that immunization of LADS-based vaccines achieved amazing effects on preventing tumor formation and growth, suggesting for the first time that the ability of LM to deliver tumor antigens makes this platform very promising in cancer immunotherapy and immunoprevention.

Vaccination of LADS-E7 altered the expression of genes related to immune function

A comprehensive exploration of genes affected by LM-based vaccine injection was performed to understand the mechanism by which LADS-E7 treatment induced potent antitumor response. C57BL/6 mice were treated with vaccines 8 and 15 days post implantation with tumor cells, and tumor tissue samples were isolated 8 days after the second vaccination and analyzed by RNA-sequencing. A total of 224 differentially expressed genes (DEGs) were identified in LADS-E7-treated group compared with LADS-injected group, among which 163 were

(See figure on next page.)

Fig. 4 Intratumoral injection of LADS-E7 generated systemic antitumor responses in established tumors. **A** Schematic illustration of the Both-side implantation experiment. Briefly, C57BL/6 J mice were subcutaneously injected with 2×10^5 TC-1 on both sides of the mouse abdomen on day 0. A total of 10^8 LADS-E7 was injected intratumorally into the tumor of one side on days 7, 12, and 17. Tumor growth was monitored on both the ipsilateral and contralateral sides. **B** Tumor growth curve of ipsilateral TC-1 tumors. **C** Growth curve of TC-1 tumors on contralateral side. **D** Frequency of E7 $tetramer^+$ $CD8^+$ T cells from tumor tissues from LADS-E7-, LADS-, and HBSS-injected mice. **E–I** Representative staining of E7 tetramer and $CD8.^+$ T cells in tumors from LADS-E7-, LADS-, and HBSS-injected mice. Tumor volume was expressed as mean ± SEM of eight mice in each group. The numbers of tumor-free mice are indicated in the figures. *$p < 0.05$, **$p < 0.01$, and ***$p < 0.001$

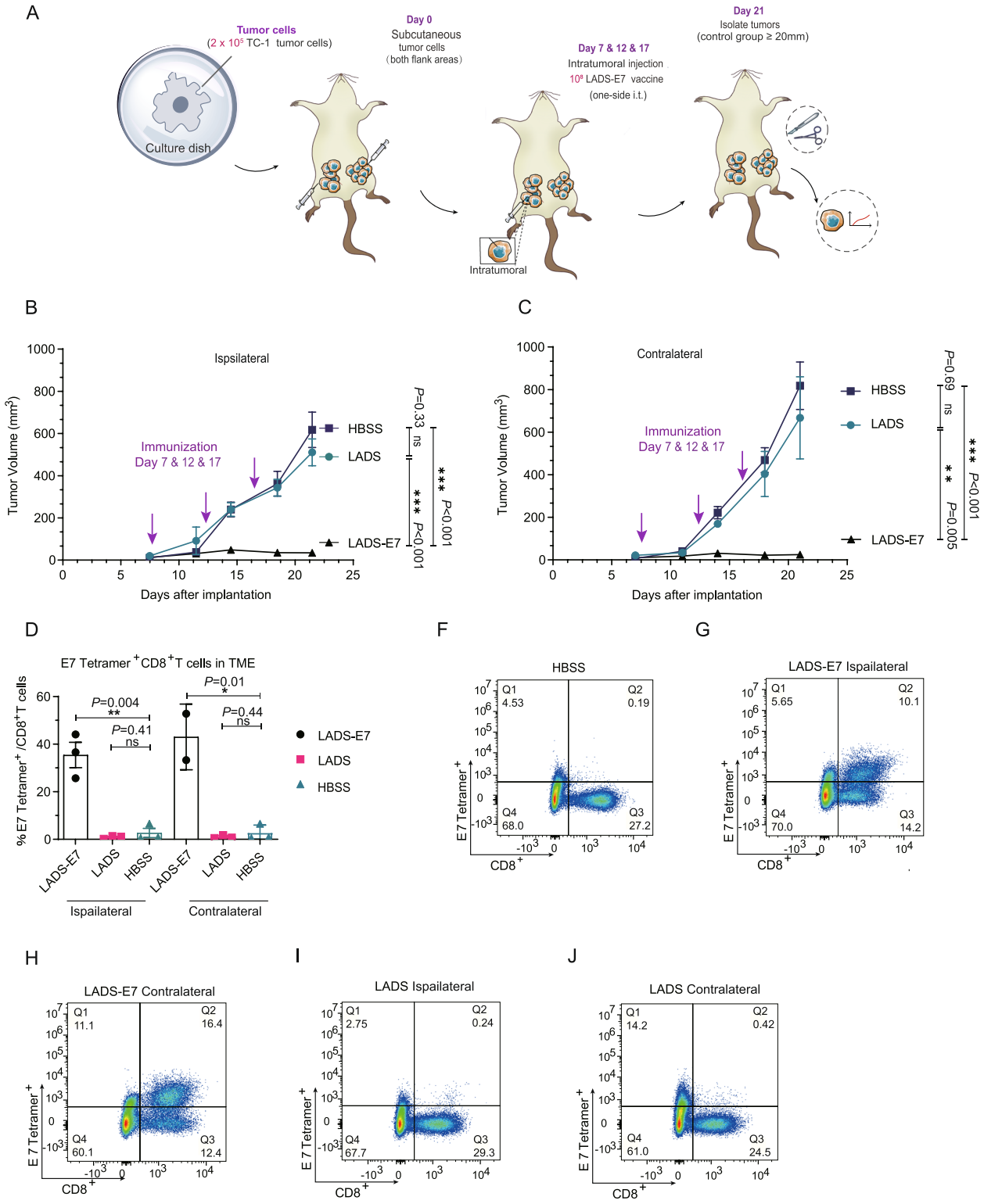

Fig. 4 (See legend on previous page.)

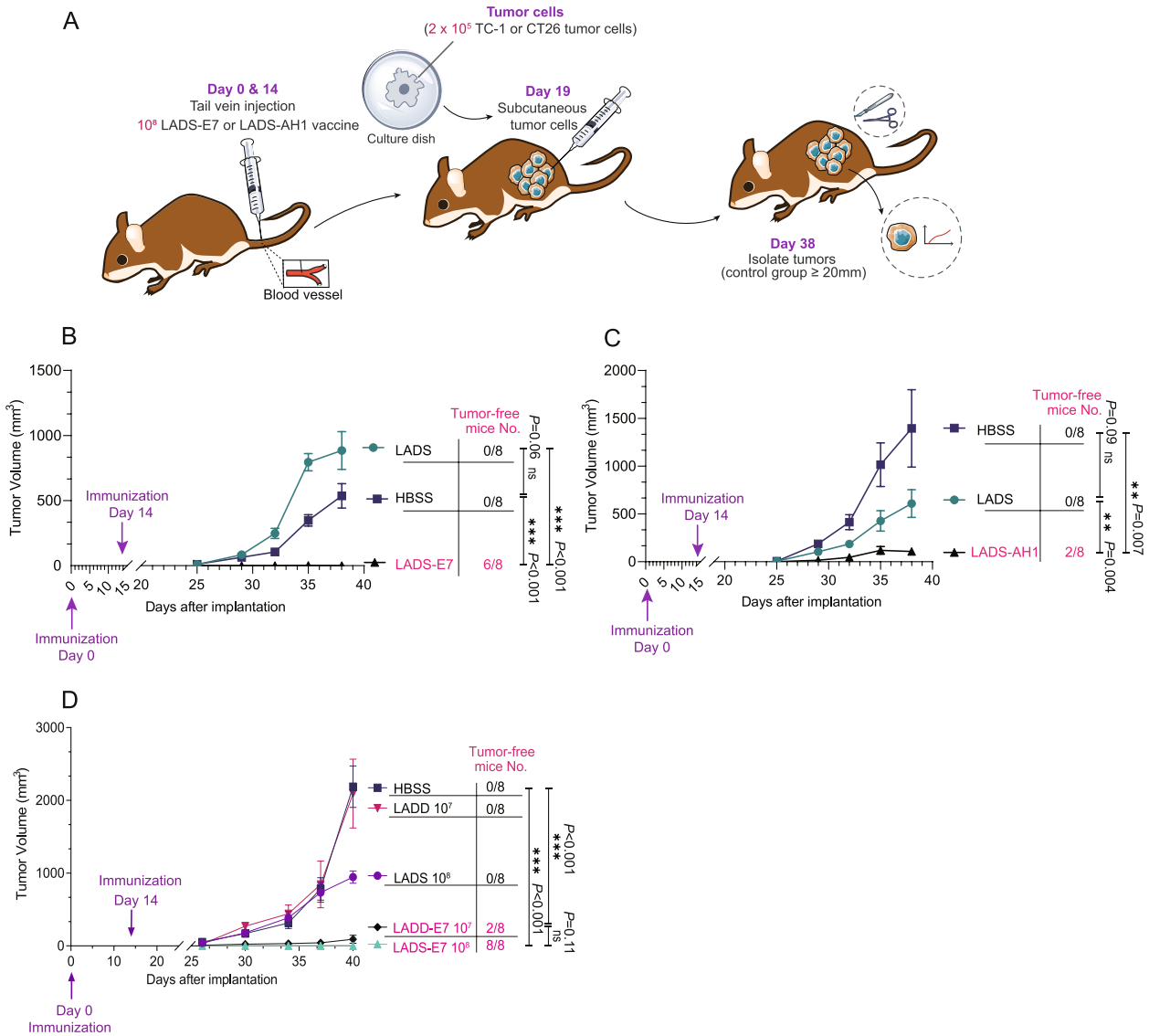

Fig. 5 Vaccination of LADS-Ag confers effective prevention of tumor implantation. **A** Schematic illustration of the tumor prevention experiment. Briefly, C57BL/6 J or BALB/c mice were immunized with LADS-E7 or LADS-AH1 on days 0 and 14, and the vaccinated mice were then implanted with $2 \times 10.^5$ TC-1 or CT26 tumor cells on day 19. The tumor formation and growth were monitored. **B** The growth of TC-1 tumors in mice vaccinated with LADS-E7 was monitored at the indicated time points. **C** The growth of CT26 tumors in mice vaccinated with LADS-AH1 was monitored at the indicated time points. **D** The growth of TC-1 tumors in mice vaccinated with LADS-E7 and LADD-E7 was monitored at the indicated time points. Tumor volume was expressed as mean ± SEM of eight mice in each group. The numbers of tumor-free mice are indicated in the figures. *$p < 0.05$, **$p < 0.01$, and ***$p < 0.001$

upregulated and 61 were downregulated (Fig. 6A, B). Five hundred eighty DEGs were detected between LADS-E7- and HBSS-injected groups, including 322 upregulated and 258 downregulated genes (Fig. 6A, B). Heatmaps indicating the differential expression of genes are demonstrated in Additional file 5: Fig. S5. Gene ontology (GO) enrichment analysis was conducted to identify the biological processes relevant to the DEGs. All top 30 GO terms are biological process and most of them are associated with immune response, including leukocyte/lymphocyte activation, innate immune response, cytokine production, leukocyte cell–cell adhesion, and leukocyte/lymphocyte aggregation (Fig. 6C). The other two GO categories, cellular component and molecular function, were also evaluated between LADS-E7 and LADS group. The result of the top 30 molecular function analysis suggested that many genes were enriched in the following GO terms: MHC protein binding, endopeptidase and

peptidase activity, and chemokine receptor binding, etc. (Additional file 6: Fig. S6). Similarly, GO analysis revealed that DEGs between LADS-E7- and HBSS-injected group were enriched in biological processes associated with immune response (Additional file 7: Fig. S7). Notably, *xcr1*, the genes encoding X-C motif chemokine receptor 1 (XCR1), were upregulated in the tumor samples from LADS-E7-treated mice compared with those from LADS- and HBSS-injected mice (Fig. 6D). XCR1 expressed on a subset of dendritic cells, which is known as type 1 conventional dendritic cells (cDC1s) and play a key role to mediate cytotoxic immune response of T cell [50–52]. In addition, *pparg*, the gene encoding transcription factor peroxisome proliferator-activated receptor gamma (PPARγ) that can enhance cytotoxic function of T cells in cancer [53–55], was upregulated in LADS-E7-injected group compared with LADS group (Fig. 6D). Furthermore, expression of genes known to enhance the antitumor cytotoxicity of $CD8^+$ T cells (such as *tlr8* and *nkg7*) [56, 57] were increased in LADS-E7-injected group (Fig. 6D). Together, these results show that LADS-E7 could affect immune response at the transcriptional level.

Discussion

The employment of LM to direct an immune response at a specific tumor burden dates back to 1995 when a study demonstrated that the use of recombinant *Listeria* could lead to the regression of established tumors in an antigen-specific T-cell-dependent manner [58]. To date, much more work has evaluated the efficient use of recombinant *Listeria* as a foreign antigen delivery platform for tumor immunotherapy in a wide range of cancer models, including breast, cervical, prostate, colon, liver, melanoma, and renal cancers [2, 3, 22, 23, 59], including 30 clinical trials testing ten different cancer vaccines initiated [9]. The unique intracellular lifestyle of LM involves phagosomal escape and cytoplasmic entry, thus giving it access to both MHC class I and II pathways as well as the consequent activation of $CD8^+$ and $CD4^+$ T cells [60], thereby making LM a promising and powerful vaccine candidate for tumor immunotherapy.

Considering that wild-type LM is pathogenic and causes listeriosis and, hence, is unacceptable for clinical use; however, there have been established strategies for attenuation that may improve the safety and maximize immunogenicity towards the target antigens delivered by *Listeria*. As reviewed to data, the selective and irreversible deletion of critical virulence factors is perhaps the most direct and conventional means of attenuating LM [61]. The most common LM vaccine strain lacking *prfA* recently demonstrated a high level of safety in Phase II clinical trials in patients with recurrent cervical cancer [62]. PrfA regulates the expression of numerous virulence factors; therefore, LM strains lacking the *prfA* gene are highly attenuated due to their inability to escape into the cytosol [63]. Another strain generated via the deletion of virulence genes *actA* and *inlB* exhibited diminished toxicity in vivo and is best known as the LADD vaccine platform. However, it has been suggested that *Listeria* virulence factors, like LLO and ActA, enhance the delivery of TAA to the proteasome, facilitating antigen processing and MHC class I presentation [25, 27]. Therefore, it is very likely that the deletion of these virulence genes can reduce the immunogenicity elicited by *Listeria* and affect cell-mediated immune responses against tumors. We described a new live attenuated vaccine platform, LADS, without depletion of any gene, only by substituting two residues on the chromosome of wild-type LM background. Using this platform, LADS-E7 and LADS-AH1 were further developed as the therapeutic vaccine candidates with impressive safety and antitumor efficacy in established mouse tumor models. More importantly, immunization of these two LADS-based vaccines achieved promising effects on preventing tumor formation and growth.

The inspiration and strategy to develop the LADS platform were originated from our previous findings that the residues N478 and V479 are required for the pore-forming activity of LLO, and complementing the *hly*-deficient mutant with $LLO_{N478AV479A}$ ($C\triangle hly_{N478AV479A}$) renders this strain severely attenuated while is still capable of growing intracellularly in macrophages and spreading cell-to-cell in fibroblasts [40]. *Listeria* has evolved mechanisms for intracellular growth and spread while minimizing cytotoxicity, largely through confining the activity of LLO to the low-pH environment of the phagosome

(See figure on next page.)

Fig. 6 Gene expression analysis of tumor tissue post LADS-E7 vaccination. Experimental procedures were same with Fig. 5A and Fig. 7A. TC-1 tumor cells were implanted into C57BL/6 mice before intravenous or intratumoral injection with LADS-E7 vaccine. Tumor tissue were isolated from mice at day 23 post implantation and subjected to RNA-sequencing analysis. **A** Venn diagram of DEGs among LADS-E7, LADS, and HBSS ($n = 1–2$, each from 2 pooled mice per group) (fold change ≥ 2 and $p < 0.05$). **B** Volcano plot of upregulated (red) and downregulated (blue) DEGs. **C** GO analysis of DEGs between LADS-E7- and LADS-treated group. **D** Heatmap comparing differential expression of immune-associated genes among LADS-E7-, LADS-, and HBSS-injected group. LADS *i.v.* and LADS *i.t.* represent the LADS vaccine were intravenous and intratumoral injected, respectively. Similarly, LADS-E7 *i.v.* and LADS-E7 *i.t.* represent the LADS-E7 were intravenous and intratumoral injected, respectively[Aikira1] [Aikira1]CE: This is unidentified paragraph from coast

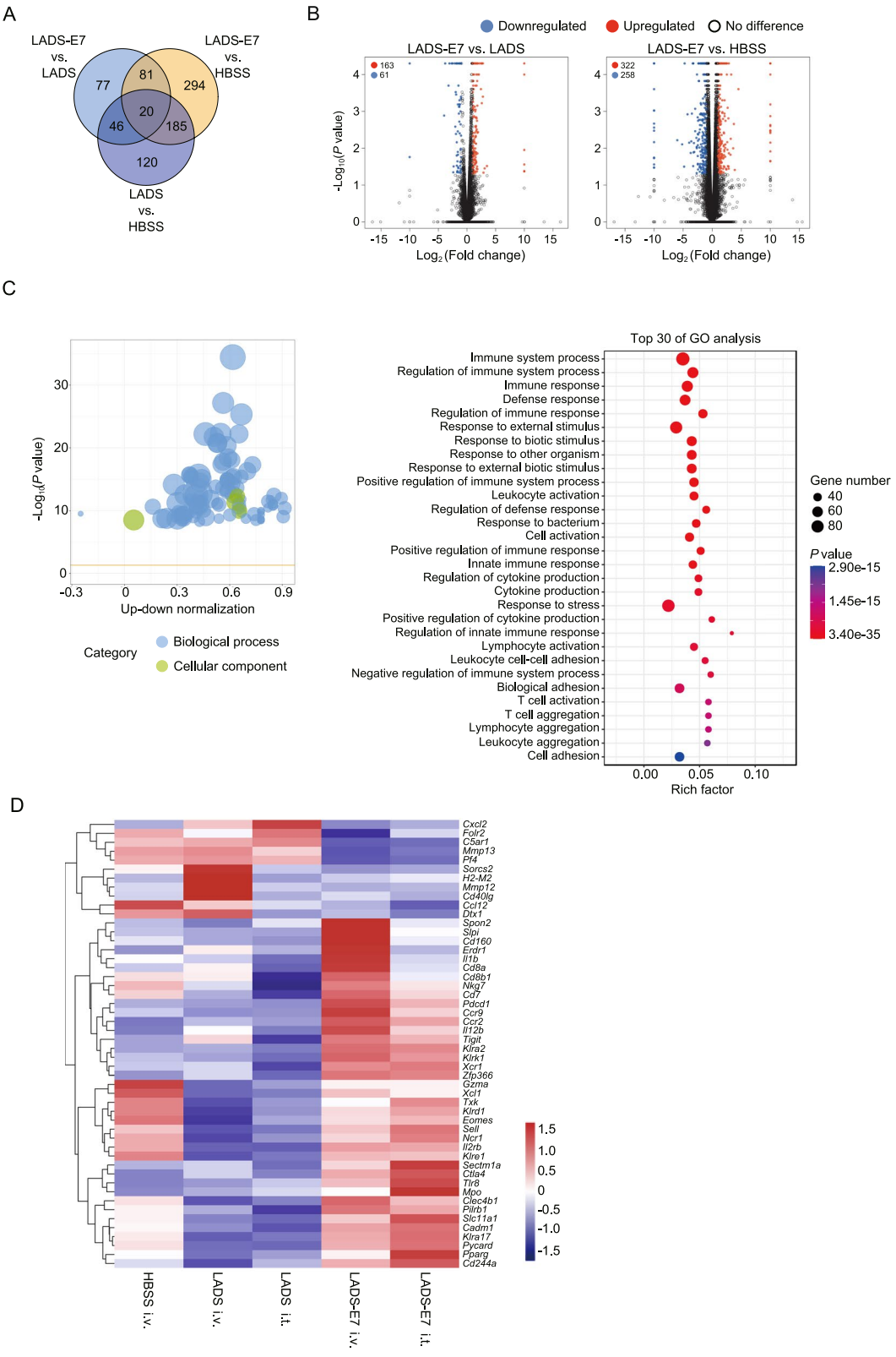

Fig. 6 (See legend on previous page.)

[20]. LLO is a pore-forming cytolysin that allows LM to escape from phagocytic vacuoles and enter the host cell cytosol [64, 65]. LLO defective mutants remain trapped in the vacuole, do not grow intracellularly, and are avirulent [66]. The previous studies have evaluated several LLO mutants with various degrees of cytotoxicity for their capacity to induce an effector immune response. Interestingly, although the LLO L461T mutant strain was highly immunogenic, the combination of that mutation with △*actA* resulted in a strain with poor immunogenicity. Other single mutants with phenotypes of increased cytotoxicity, including △PEST, and S44A, were considerably impaired in their capacity to induce a primary immune response [20, 67]. Therefore, how to get an LLO mutant with the "just right" cytotoxicity and complete immunogenicity is particularly critical for *Listeria* as a perfect platform in cancer immunotherapy. In this study, we introduced this mutation ($LLO_{N478AV479A}$) into the chromosome of the wild-type LM EGD-e, receiving the recombinant strain LADS. Our results collectively indicated that the LD50 for LADS is $10^{9.07}$ CFUs in a mouse model compared to $10^{5.25}$ CFUs by wild-type LM while retaining perfect protective immunogenicity, demonstrating that the attenuated LADS meets the safety and immunogenicity requirements as a promising live vaccine. Furthermore, we compared the safety of LADS-E7 and LADD-E7, which was generated by employing the most widely used attenuated LADD platform through a similar strategy of LADS-E7 construction. Surprisingly, LADS-E7 showed higher LD50 value when compared with LADD-E7 and is safer for potential use as a live vaccine vector (Additional file 2: Fig. S2D, E). Additionally, C57BL/6 J mice infected with 0.1 LD50 of LADS were able to completely clear the bacteria in 6 days post-infection. Importantly, bacterial delivery systems carrying antibiotic resistance marker-contained plasmids have been discouraged in clinical applications by the Food and Drug Administration of the United States because of the associated potential risk of environmental spread [68]. LADS was constructed by only introducing an in situ substitution on LLO residues, without any foreign plasmids. Hence, from the aspect of safety, LADS that is free of antibiotic resistance markers to conform to clinical regulatory requirements and improve environmental safety, is more suitable for becoming a powerful live bacterial vaccine vector.

Undoubtedly, antigens have always been the core focus of design for cancer vaccines. Viral antigens and neoantigens are considered ideal targets because of the lack of central tolerance [69]. The preclinical potency of LM expressing the viral antigens AH1 and E7 highlights the therapeutic potential of targeting these antigens [26, 70]. To test the potential applications of this new platform in tumor immunotherapy, we further developed two LADS-based vaccine candidates, LADS-E7 and LADS-AH1, in either which the tumor antigen was genetically fused to the carboxyl-terminal of $LLO_{N478AV479A}$, a partially detoxified form of LLO (pdLLO) as previously determined [40]. Many studies have shown that the fusion of tumor-associated antigen to a nonfunctional LLO significantly enhances the immunogenicity of the target antigen and the efficacy of the cancer immunotherapy [13, 17, 27, 71]. One of these studies reported that LM expressing E7 alone had almost no effect on tumor growth, but immunization with dtLLO-E7-expressing LM-induced complete regression of 75% of the tumors [17]. Here, the LADS vaccine was found to express and secrete $LLO_{N478AV479A}$ that retains partial hemolytic activity. Therefore, we believe that $LLO_{N478AV479A}$ is also a powerful adjuvant that enhances TAA delivery and facilitates antigen processing and MHC presentation. To test adjuvant properties of dtLLO, LADS-E7 and LADS-AH1 were finally evaluated in mice models for the potential potency as therapeutic vaccines. It is very encouraging that treatment or immunization with LADS-E7/AH1 significantly delayed or completely prevented tumor growth and even led to complete regression of established tumors. Additionally, intratumoral vaccination of LADS-based vaccines can generate systemic antitumor responses to control distant tumor growth. Surprisingly, immunization with 0.1 LD50 of LADS-E7 can mediate the elimination of tumor cells in all mice, whereas injection of the mice with 0.1 LD50 of LADD-E7 cannot protect the mice from tumor development (Fig. 5D). These demonstrate that LADS can become a powerful platform for the future development of both immunotherapeutic and preventive vaccines against cancers and infectious diseases.

It has been widely understood that LM is rapidly taken up by immune cells such as dendritic cells and macrophages upon entering the host. Because of this bacterium's unique intracellular lifestyle, an antigen expressed by the LM-based vaccine can be presented. As a result, the cellular immune response elicited against these antigens includes both $CD4^+$ and $CD8^+$ T cells. We observed that the LADS vector alone was sufficient to increase $CD4^+$ and $CD8^+$ T-cell numbers. However, with fusion expression to a dtLLO, immunization with LADS-E7/AH1 resulted in a significant increase in the population of E7/AH1-specific $CD8^+$ T cells in spleens and tumors as compared to control mice. Thus, the increase of tumor antigen-specific $CD8^+$ T cells derived by LADS-based vaccine might be due to the efficient presentation of TAAs by macrophage and dendritic cells. Interestingly, our RNA-sequencing result showed that LADS-E7 treatment upregulated the expression of XCR1 in tumor

tissue samples (Fig. 6D), which implies that dendritic cell-mediated T cell antitumor response was enhanced in LADS-E7-injected mice. XCR1 is a chemokine receptor expressed by cDC1 cells, which play a crucial role inducing cellular immune response against intracellular infection and cancer through optimal processing and cross-presentation of antigen to activate $CD8^+$ T cells [50–52]. Additionally, XCR1 expressing cDC1 cells prime and support the immune response of Th1 cells, which can further favor cytotoxic $CD8^+$ T cell response [51, 52, 72]. However, a lot of immunosuppressive factors enriched in the TME hamper the differentiation, activation, and viability of cDC1 cells, resulting in impaired antigen presenting capacity and reduced pro-inflammatory cytokines production and, subsequently, the inefficient priming of tumor-specific T cell response [51, 52]. On the other hand, the increase of cDC1s cells in TME is associated with improved prognosis in human tumor [50, 51]. Thus, targeting dendritic cells to induce robust antitumor T cell response is an attractive strategy for cancer immunotherapy [50, 51, 73]. Previous studies have reported that LM can induce functional maturation and activation of dendritic cells with high expression of costimulatory molecules and cytokines, leading to efficient priming of antigen-specific T cell response [8, 16, 74, 75]. Meanwhile, GO analysis in this study showed that a lot of DEGs were enriched in the significant GO terms, including leukocyte/lymphocyte activation, leukocyte cell–cell adhesion, MHC protein binding, endopeptidase, and peptidase activity (Fig. 6C and Additional file 6: Fig. S6), which might imply that antigen processing and presentation were enhanced in LADS-E7-injected mice. Therefore, the superior antitumor response after LADS-E7 treatment might be partly due to the increased XCR1 expressing cDC1 cells loaded with TAAs that can prime the antitumor T cell response. It is intriguing to test in the future whether LADS-E7 can enhance the generation of cDC1 cells in tumor-draining lymph nodes and TME. Additionally, the link between cDC1 cells and the efficient tumor regression in this study need to be examined.

The gene expression level of transcription factor PPARγ in tumor tissue was higher in the LADS-E7-treated mice than other control mice (Fig. 6D). The activation of PPARγ promote fatty acid oxidation and mitochondrial respiratory capacity of $CD8^+$ T cells in TME leading to enhanced cytotoxic function and increased survival capacity [53–55]. In dendritic cells, PPARγ are involved in maturation, activation, antigen presentation, and cytokine production through regulation of lipid metabolism [76, 77]. Furthermore, PPARγ has been shown to play an important role for the full activation and proliferation of $CD4^+$ T cells by regulating fatty acid uptake [54, 78]. However, PPARγ activation can also drive the differentiation of M2 macrophages (a subset of macrophage display anti-inflammatory activity) which rather suppress the cytotoxic function of T cells [79–81]. It will be necessary to examine how LADS-E7 affects the expression of PPARγ, and whether this upregulated transcription factor is responsible for the promoted antitumor response.

Treatment with LADS vaccines significantly suppressed Tregs frequency in the tumor infiltrated lymphocyte population. Tregs consist of functionally diverse subsets of immune suppressive T cells that mediate the modulation of immune responses and participate in the progression of cancers [82, 83]. It has been clear that Tregs are significantly decreased upon administration of LM-based vaccines that secrete TAAs fused to truncated LLO compared to those secreted the TAA alone [7, 84]. There are mainly three approaches to reduce the accumulation of Tregs in the TME: blockade of their recruitment, inhibition of their induction, and supporting their differentiation into other $CD4^+$ T cell subsets [85, 86]. The mechanism of how LADS-based vaccine affects Tregs in the TME need to be further examined. Taken together, we have provided novel evidence demonstrating that fusion expression of a partially detoxified LLO to the TAA in the LADS platform preferentially triggered a dramatic increase of tumor-specific $CD8^+$ T cells and decrease of Tregs proportions, thereby generating strong tumor regression and prevention effects as a powerful cancer vaccine (Fig. 7).

Conclusions

In summary, our study developed a novel live attenuated *Listeria*-based vaccine delivery platform, LADS, and it has been successfully employed to deliver HPV E7 oncoprotein in the LADS-E7 vaccine and the AH1 antigen in LADS-AH1. These two LADS-based vaccines can induce robust cell-mediated immune responses, thereby demonstrating promising tumor regression efficacy in established mouse cervical cancer and colorectal carcinoma models. Moreover, the intratumoral injection of these vaccines can also generate strong antitumor responses both locally and systemically. In the future work, we will aim to use the LADS platform to develop more vaccine candidates for tumor immunotherapy and immunoprevention against a wide range of cancer models, and more importantly, to explore new strategies for the synergism of these novel *Listeria*-based vaccines in combined with immune checkpoint blockade and other cancer therapy strategies.

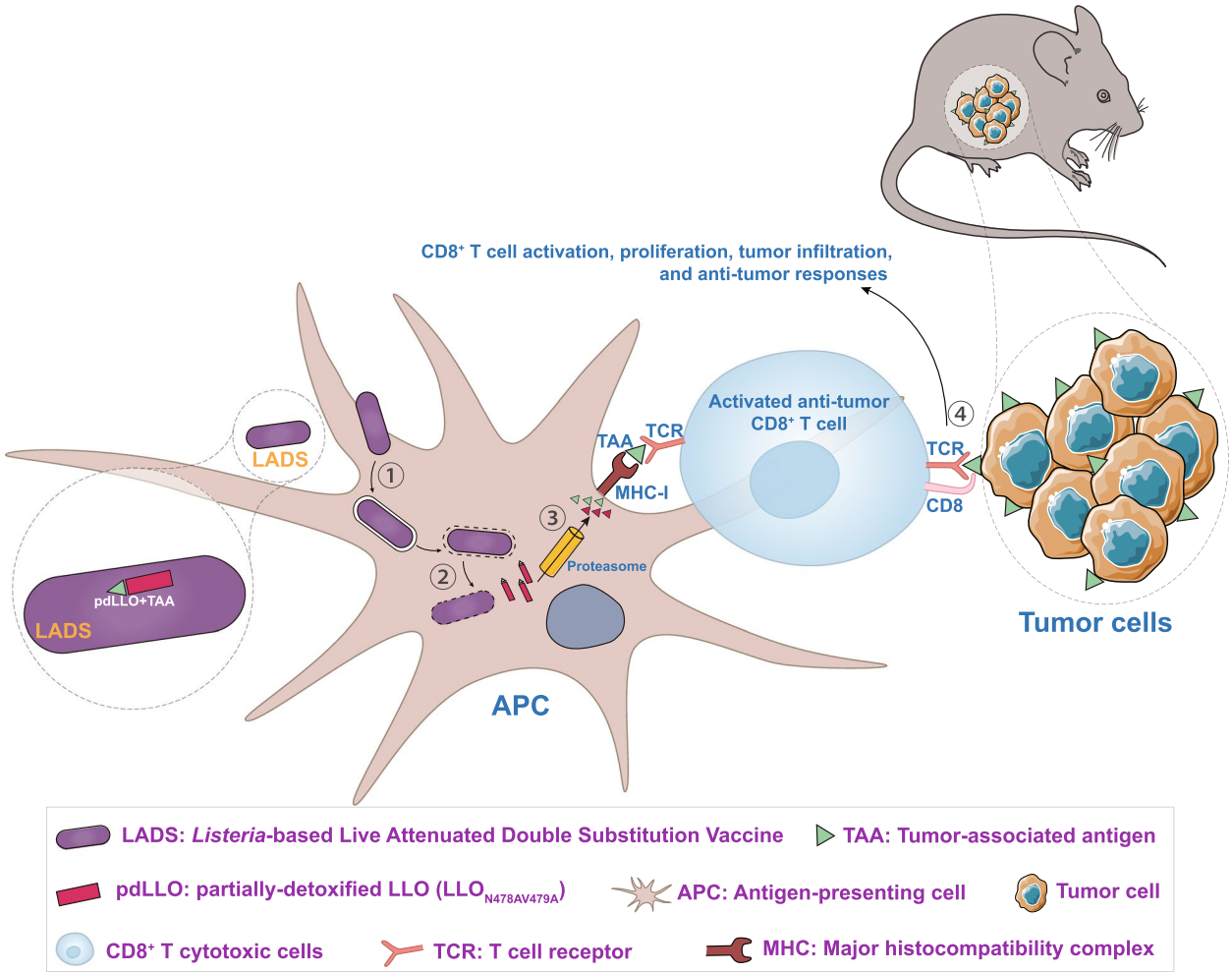

Fig. 7 A model depicting mechanisms of LADS-based vaccine for cancer immunotherapy and prevention. The novel *Listeria*-based Live Attenuated Double Substitution (LADS), developed by genetically substituting two residues (N478A and V479A) of LLO, was here employed as a potential vector for delivering tumor-associated antigen (TAA). (1) Upon intravenous administration, LADS-based vaccines are internalized by antigen-presenting cells (APC), such as dendritic cells. (2) LADS-based vaccines escape the phagosome, enter the cytosol, replicate, and secrete TAAs fused to the partially detoxified $LLO_{N478AV479A}$ (pdLLO-TAA). (3) Secreted fusion proteins are degraded by proteasomes, followed by entering the major histocompatibility complex (MHC) class I pathway of antigen presentation for activation of TAA-specific $CD8^+$ cytotoxic T cells. (4) The activated TAA-specific $CD8^+$ T cells undergo rapid proliferation and tumor infiltration, generating strong cellular immune responses to directly kill tumor cells (or prevent tumor formation if used as a preventive vaccine). As not indicated, part of the antigens from the vacuole is processed via the MHC class II molecules which activate $CD4^+$ helper T cells. These unique features of *Listeria*-based vaccines with impressive efficacy make LADS powerful for tumor immunotherapy and prevention as an attractive foreign antigen-delivering platform

Methods

Mice

Female C57BL/6 J and BALB/c mice (6–8 weeks old) were bred by and purchased from Zhejiang Academy of Medical Sciences. All animal experimentation was approved by the Institutional Animal Care and Use Committee of Science Technology Department of Zhejiang Province (Permit Number: SYXK-2023–0015) in accordance with the Regulations for the Administration of Affairs Concerning Experimental Animals. In this study, the euthanasia method for tumor-bearing mice involved cervical dislocation, a physical approach performed directly within the laboratory. This method did not require special equipment or animal transportation. Following the experiments, the mice were disposed of in a biologically safe manner. All the tumor-bearing mice weighed less than 200 g, meeting the study's requirements. The personnel conducting the euthanasia were trained and highly proficient in animal euthanasia techniques. Our euthanasia procedures strictly adhered to the "AVMA Guidelines for the Euthanasia of Animals: 2020 Edition".

Cell lines

The C57BL/6 J mice syngeneic TC-1 tumor cells, immortalized with HPV strain 16 E6/E7 antigens and transformed with the c-Ha-*ras* oncogene [87], and the BALB/c mice colorectal carcinoma cell line CT26, were purchased from the Tumor Cell Center of the Chinese Academy of Medical Sciences (Beijing, China). TC-1 and CT26 cells were cultured in RPMI 1640, supplemented with 10% fetal bovine serum (FBS), 1 mM sodium pyruvate, 100 U/mL penicillin, and 100 μg/mL streptomycin at 37 °C with 5% CO_2. The macrophages RAW264.7 and J774A.1 and the L929 fibroblasts were maintained in our laboratory and cultured according to regular protocols. The BMDMs were derived from the bone marrow of C57BL/6 J mice and cultivated/differentiated in high-glucose DMEM medium containing colony stimulating factor (CSF) (from mouse CSF-1-producing 3T3 cells), 20% FBS, 2 mM L-glutamine, and 1 mM sodium pyruvate 37 °C with 5% CO_2.

Bacterial strains, plasmids, and culture conditions

LM EGD-e was used as the wild-type strain. *E. coli* DH5α was employed for cloning experiments and as the host strain for plasmid pKSV7. LM strains were cultured in Brain Heart Infusion (BHI) medium (Thermo Fisher Scientific, Waltham, USA). *E. coli* strains were grown at 37 °C in Luria–Bertani broth (LB) (Thermo Fisher Scientific). Stock solutions of ampicillin (50 mg/mL), gentamycin (10 mg/mL), or chloramphenicol (10 mg/mL) were added to the medium where appropriate. All chemicals were obtained from Sangon Biotech (Shanghai, China), Thermo Fisher, or Sigma-Aldrich (St. Louis, USA) and were of the highest purity available.

Construction of LADS-based vaccinesLADS-E7 and LADS-AH1

As we have previously demonstrated that the residues Asn478 and Val479 are new active sites required for LLO activity and bacterial pathogenicity [40], the novel live-attenuated LM immunotherapy platform LADS was constructed on the reference strain EGD-e background by introducing this mutation $LLO_{N478AV479A}$ into the EGD-e chromosome. As LADS-E7 an example, the complete protein-encoding region of the HPV 16 E7 gene was introduced into LADS as a fusion protein in-frame with $LLO_{N478AV479A}$ by allelic exchange. Specifically, the upstream and downstream homoarm fragments (LLOup and LLOdn) were amplified from the LADS genome using the primers as indicated in Additional file 8: Table S1. The resultant fragments were spliced by overlap extension PCR with the primers LLOup (F) and LLOdn (R), and the fusion fragment was then cloned into the shuttle vector pKSV7. The resulting recombinant plasmid was electroporated into competent EGD-e cells. A single colony of the construct was grown at non-permissive temperature (42 °C) on BHI agar containing chloramphenicol to promote chromosomal integration. After that, the recombinants were successfully passaged without antibiotics at a permissive temperature (30 °C) to enable plasmid excision and curing. The successful construction of the LADS-E7 strain was finally confirmed by Sanger DNA sequencing. Similarly, the gene encoding AH1 epitope (amino acid residues 423–431, SPSYVYHQF) [37] was introduced into LADS to construct LADS-AH1 by using its specific primers (Additional file 8: Table S1).

Secretion of the $LLO_{N478AV479A}$-Ag fusion protein by LADS-Ag

Overnight-grown LADS-Ag bacteria were separated from the culture medium by centrifugation at 10,000 *g* for 10 min, and the supernatants recovered [88–90]. Briefly, the culture medium was collected after the initial centrifugation and filtered through a 0.22-μm sterile filter to eliminate any bacteria that might be present. To obtain the secreted proteins, the proteins in the filtered supernatant were precipitated in the presence of 10% v/v trichloroacetic acid (TCA) on ice overnight, and the precipitated proteins were washed twice with ice-cold acetone. Precipitates of supernatant proteins were then re-suspended in SDS-PAGE sample buffer and separated on a 12% gel by SDS-PAGE. After transferring the proteins onto PVDF membranes, the fusion protein $LLO_{N478AV479A}$-Ag was detected by immunoblotting with either a monoclonal anti-TAA (Anti-human papillomavirus 16 (E7) antibody (289–17,013, TVG-701Y), Abcam, Cambridge, UK) or a polyclonal anti-LLO antibody. The immunoreactions were carried out using the ECL detection kit (Pierce, Rockford, IL, USA) and signals visualized using the enhanced chemiluminescence detection system (UVP Inc., Upland, USA).

LLO-mediated hemolytic analysis

Measurement of LLO-associated hemolytic activity was performed as previously described [91]. Briefly, strains of LM were grown for 12 h with shaking in BHI broth at 37 °C. All cultures were adjusted to an OD_{600} of 1.0 before supernatant protein samples were collected. Hemolytic activity was measured based on sheep red blood cells (SRBCs) lysis by secreted LLO from culture supernatants. Specifically, culture supernatant (50 μL) was diluted in an equal volume of hemolysis buffer (10 mM PBS, pH 5.5 or 7.4, 150 mM NaCl, 1 mM DTT), and equilibrated to 37 °C for 10 min. Next, 100 μL PBS-washed intact SRBCs (5%) were added to each sample and incubated at 37 °C for 30 min. Samples were centrifuged, and supernatants

were analyzed for hemoglobin absorption at 550 nm. Erythrocytes incubated with 1% Triton X-100 or PBS served to determine the maximum (100%) and minimum (0%) hemolytic activity, respectively.

Intracellular growth in RAW264.7 and J774A.1 macrophage

Intracellular growth was performed accordingly on RAW264.7 or J774A.1 macrophages. Specifically, monolayers of macrophages were cultured in DMEM medium containing 20% FBS and plated in 24-well plates that contained 2×10^5 cells per well. Cells were then infected with bacteria at an MOI of about 0.25 for 30 min, washed twice with warmed PBS prior to replacing media, and added gentamycin at 50 μg/mL 1 h post-infection. At 2, 6, or 12 h post-infection, cells were lysed in sterile water, and the lysates were tenfold serially diluted for enumeration of viable bacteria by plating on BHI agar.

Intracellular growth in BMDMs

Growth curves in BMDMs were performed as previously described with minor modifications [66, 92]. Briefly, BMDMs were plated in 24-well plates with 2×10^5 cells per well and infected at an MOI of about 0.25 for 30 min, washed twice with PBS prior to replacing media, and gentamycin was added at 50 μg/mL 1 h post-infection. At 0.5, 2, 5, and 8 h post-infection, cells were lysed in sterile water, and the lysates were tenfold serially diluted for enumeration of viable bacteria by plating on BHI agar.

Virulence in the mouse model

LM wild-type strain EGD-e and vaccine strain LADS were tested for virulence in mice models. For the determination of bacterial burdens in organs, ICR mice (8 per group) were injected intraperitoneally with ~ 10^6 CFU of each strain. At 24- and 48-h post-infection, mice were sacrificed, and livers and spleens removed and individually homogenized in 10 mM PBS (pH 7.4). Surviving bacteria were enumerated by plating serial dilutions of homogenates on BHI agar plates. Results were expressed as means ± SEMs of recovery bacterial number (Log10 CFU) per organ for each group. To determine the LD50, ICR mice injected intraperitoneally with $10^4 \sim 10^9$ CFU of each *Listeria* strain were monitored over 10 days. The LD50 of the challenge strains was calculated by the method of Reed and Muench. For the clearance and efficacy test of LADS in organs, C57BL/6 J mice were injected intravenously with ~ 10^8 CFU LADS. At 2, 3, 4, 5, or 6 days post-infection, six mice (from two independent experiments) of each group were sacrificed, and livers and spleens were removed and individually homogenized in 10 mM PBS (pH 7.4). Surviving bacteria were enumerated by plating serial dilutions of homogenates on BHI agar plates. Results were expressed as means ± SEMs of recovery bacterial CFUs per organ.

Tumor-immunotherapy and tumor-prevention studies

To establish tumor models, C57BL/6 J or BALB/c mice were subcutaneously injected with 2×10^5 TC-1 or CT26 cells on the left flank, respectively. For tumor immunotherapeutic experiments, tumor-bearing mice were randomly administered with 0.1 LD50 of LADS, or LADS-E7/AH1 in a total volume of 100 μL by intravenous injection or intratumoral injection after the tumors had reached a palpable size of 4–5 mm in diameter. C57BL/6 J or BALB/c mice were immunized with LADS-E7 or LADS-AH1 on days 0 and 14 by tail vein injection for tumor prevention experiment. Five days post last immunization, the vaccinated mice were subcutaneously implanted with 2×10^5 TC-1 or CT26 tumor cells on the left flank.

Mice immunized with HBSS or LADS were used as the negative or background control. Tumor growth was monitored, tumor size was measured twice a week with an electronic caliper, and the widest (W) and longest (L) surface diameters were recorded for each individual tumor. Tumor volume was calculated as $L\times W^2/2$. Mice were sacrificed when the tumor size reached a 20-mm average diameter.

Flow cytometric analysis of $CD4^+$, $CD8^+$ T, and Treg cells

C57BL/6 J or BALB/c mice were implanted with 2×10^5 TC-1 or CT26 tumor cells on the left flank as described above. The tumor-bearing mice were immunized *i.v.* on days 8 and 15 after tumor challenge with 0.1 LD50 of LADS, LADS-E7/AH1, or HBSS as a control. On day 18, tumors and spleens were then harvested from two or three mice and cut into 1–2-mm pieces using a sterile razor blade and digested with PBS buffer containing 2 mg/mL collagenase type I and 12 U/mL DNase (Thermo Fisher Scientific, Waltham, USA) for 2 h at 37 °C with agitation. Single-cell suspensions were pooled through a nylon mesh. Cells were stained with anti-CD3-fluorescein isothiocyanate (FITC) (clone 145-2C11; BD Biosciences-Pharmingen, San Diego, CA), anti-CD4-phycoerythrin (PE) (clone RM4-5; BD Biosciences-Pharmingen), anti-CD8-allophycocyanin (APC) (clone 53–6.7; BD Biosciences-Pharmingen); anti-CD4-FITC (clone RM4-5; BD Biosciences-Pharmingen), anti-CD25-APC (clone PC61; BD Biosciences-Pharmingen), anti-FoxP3-PE (clone R16-715; BD Biosciences-Pharmingen) monoclonal antibodies, and H-$2D^b$ E7 (RAHYNIVTF) tetramer-PE (TB-5008–1, MBL Beijing Biotech, China), and H-$2L^d$ MuLV gp70 (SPSYVYHQF) tetramer-PE (TS-M521-1, MBL Beijing Biotech) for 30 min, and then subjected to multicolor flow cytometry using a FACSCelesta flow cytometer with FlowJo software (BD Biosciences-Pharmingen),

according to the manufactures' instructions. Tregs were defined as $CD4^+CD25^+Foxp3^+$ cells.

RNA-sequencing analysis

The total RNA was extracted from the tumor tissues of two mice per group following the manufacturer's instructions of the TRIzol reagent kit (Invitrogen, Carlsbad, CA). RNA sequencing analysis was performed by the contract service of MK-bio Mingke Biotechnology Co., Ltd. (Hangzhou, China). RNA quality was examined through 2100 Bioanalyser (Agilent, Waldbronn, Germany) and quantified using the ND-2000 (NanoDrop Technologies, Wilmington, DE). RNA-seq transcriptome libraries were prepared from the total RNA using the TruSeqTM RNA sample prep Kit (Illumina, San Diego, CA). The raw paired end reads were trimmed and quality controlled by Trimmomatic (version 0.40), then clean reads were separately aligned to reference genome (mm10) using tophat (version 2.0.0). The expression level of each transcript was calculated using fragments per kilobase of exon per million mapped reads (FRKM). Differential expression analysis was performed through Cuffdiff (version 0.0.5), and the genes exhibiting two-fold or higher expression differences ($P < 0.05$) between the groups were extracted. GO analysis was performed by OmicShare online tools (version 3.14.0) to understand the functions of the DEGs.

Abbreviations

APC	Allophycocyanin
BMDMs	Bone marrow-derived macrophages
BHI	Brain Heart Infusion
CTL	Cytotoxic T lymphocytes
CSF	Colony-stimulating factor
cDC1s	Type 1 conventional dendritic cells
DEGs	Differential expression genes
FBS	Fetal bovine serum
FITC	Fluorescein isothiocyanate
GO	Gene ontology
gp70	Glycoprotein 70
HPV	Human papillomavirus
HBSS	Hanks' Balanced Salt Solution
IL	Interleukin
IFN	Interferon
LM	*Listeria monocytogenes*
LADS	*Listeria*-Based Live Attenuated Double Substitution
LLO	Listeriolysin O
LADD	Live Attenuated Double-Deleted
Lmdd	Δ*dal*/Δ*dat* Strain
LB	Luria-Bertani
LD50	Median lethal dose
MHC	Major histocompatibility complex
PE	Phycoerythrin
PPARγ	Peroxisome proliferator-activated receptor gamma
pdLLO	Partially detoxified form of LLO
SRBCs	Sheep red blood cells
Tregs	Regulatory T cells
TAA	Tumor-associated antigens
TLR4	Toll-like receptor 4
Th1	Type 1 helper
TCA	Trichloroacetic acid
TME	Tumor microenvironment
XCR1	X-C motif chemokine receptor 1

Supplementary Information

The online version contains supplementary material available at https://doi.org/10.1186/s12915-024-02086-7.

Additional file 1: Fig. S1. LADS secreting $LLO_{N478AV479A}$ with impaired hemolytic activity is unable to grow intracellularly in macrophages.The construction strategy of LADS by introducing the substitution mutation-into the wild-type LM.Expression and secretion of LLO or $LLO_{N478AV479A}$ from wild-type, LADS, or LLO-deletionLM was detected by immunoblotting anti-LLO polyclonal antibody, with GAPDH or the extracellular protein p60 [94] as the internal control for cytoplasmic or secreted proteins, respectively.In vitro growth of wild-type, LADS, or Δ*hly* in BHI medium. Kinetic growth at $OD_{600\ nm}$ was measured at 1-h intervals. Data are expressed as mean ± SEM of three replicates.Hemolytic activity of secreted LLO from culture supernatants of wild-type, LADS, or Δ*hly* LM. Erythrocytes incubated with 1% Triton X-100 or PBS served to determine the maximumand minimumhemolytic activity, respectively.Intracellular growth of wild-type, LADS, or Δ*hly* bacteria in J77A4.1, RAW264.7, and BMDM. The infected macrophages were lysed at the indicated time points, and viable bacteria were serially plated on BHI plates. All the data are expressed as mean ± SEM of three replicates. $*p < 0.05$, $**p < 0.01$ and $***p < 0.001$. α-LLO, α-p60 and α-GAPDH represent the anti-LLO, anti-p60 and anti-GAPDH antibodies, respectively.

Additional file 2: Fig. S2. LADS is highly attenuated for the virulence in a mouse model. The Kaplan–Meier curves of the survival of the ICR mice infected with LADS (A), wild-type (B), Δ*hly* (C), LADS-E7 (D) or LADD-E7 (E) LM with various bacterial concentrations. Ten mice in each experimental group were injected intraperitoneally with each concentration of bacterial CFUs as indicated and monitored for up to 7 days after infection. Data are presented as the percentage survival over time, and the indicated LD50 values of the challenge strains were calculated by the method of Reed and Muench. (F-G) The proliferation of LM in mice organs (liver and spleen). The wild-type or LADS bacteria were inoculated intraperitoneally into ICR mice at ~ 4×10^6 CFU. Animals were euthanized at 24 (F) or 48 (G) h post-infection, and organs (livers and spleens) were recovered and homogenized. Homogenates were serially diluted and plated on BHI agar. The numbers of bacteria colonizing the organs are expressed as mean ± SEM of the $\log_{10}$CFU per organ for each group (7 mice). (H) Kinetics of LADS clearance in the mice organs. The C57BL/6 J mice were injected intravenously with ~ 10^8 CFU LADS bacteria. Six mice per group from two independent experiments were sacrificed at 2, 3, 4, 5, or 6 days post-infection, and bacteria isolated from livers and spleens were enumerated as described above. Data were expressed as means ± SEMs of recovery bacterial CFUs per organ.

Additional file 3: Fig. S3. The LADS-E7/AH1 can secrete the fused $LLO_{N478AV479A}$-E7/AH1 antigen. (A) The construction strategy of LADS-based vaccines by introducing the HPV type 16-derived E7 antigen or the murine colon carcinoma AH1 antigen with a fusion to $LLO_{N478AV479A}$ in the LADS genome. (B-C) Expression and secretion of $LLO_{N478AV479A}$, $LLO_{N478AV479A}$-E7 (B), or $LLO_{N478AV479A}$-AH1 (C) from LADS, LADS-E7, or LADS-AH1 bacteria. The interest proteins were detected by immunoblotting using anti-TAA or LLO antibodies, with GAPDH or p60 as the internal control for secreted or cytoplasmic proteins. (D) In vitro growth of LADS, LADS-E7, or LADS-AH1 in BHI medium. Kinetic growth at $OD_{600\ nm}$ was measured at 1-h intervals. Data are expressed as mean ± SEM of three replicates. (E) Hemolytic activity of secreted LLO from culture supernatants of wild-type, LADS, LADS-E7, or LADS-AH1 bacteria. Erythrocytes incubated with 1% Triton X-100 or PBS served to determine the maximum (100%) and minimum (0%) hemolytic activity, respectively. All the data are expressed as mean ± SEM of three replicates. $*p < 0.05$, $**p < 0.01$ and $***p < 0.001$. α-E7, α-LLO, α-p60 and α-GAPDH represent the anti-E7, anti-LLO, anti-p60 and anti-GAPDH antibodies, respectively.

Additional file 4: Fig. S4. The flow cytometry gating strategy flow chart

Additional file 5: Fig. S5. Heatmap of DEGs in tumor samples between LADS-E7 and LADS treated mice (fold change ≥ 2 and $p < 0.05$). *i.v.* and *i.t.* represent the vaccine were intravenous and intratumoral injected, respectively.

Additional file 6: Fig. S6. GO molecular function analysis of DEGs in tumor tissue between LADS-E7 and LADS injected mice

Additional file 7: Fig. S7. GO analysis of DEGs between LADS-E7 and HBSS injected group

Additional file 8: Table S1. Primer List. The PCR primers used in this study

Additional file 9: Images of the original, uncropped gels/blots

Acknowledgements
We would like to express our sincere thanks to all the authors for their contributions to the study.

Authors' contribution
C.C., and H.S. conceived of the study. C.C., J.S., X.J., J.W., J.X.1, Y.H., and M.C performed all the experiments. C.C., S.D., and J.X.2 analyzed the data. C.C. and J.S wrote and revised the manuscript, with J.X.1 corresponding to Jing Xia, with J.X.2 corresponding to Jiali Xu. All authors read and approved the final manuscript.

Funding
This study was supported by the National Key R&D Program of China (No. 2023YFD1801800), the Natural Science Foundation of Zhejiang Province (LY23C180002 and LY24C180001), and the National Natural Science Foundation of China (32473026, 32172849, and 32302961).

Availability of data and materials
The authors confirm that the data supporting the findings of this study are available within the article and its supplementary materials. The RNA-seq data were deposited in NCBI under accession number PRJNA1190894 (BioProject ID) [93].
No datasets were generated or analysed during the current study.

Declarations

Ethics approval and consent to participate
All animal experimentation was approved by the Institutional Animal Care and Use Committee of Science Technology Department of Zhejiang Province (Permit Number: SYXK-2023–0015) in accordance with the Regulations for the Administration of Affairs Concerning Experimental Animals.

Consent for publication
N/A.

Competing interests
The authors declare no competing interests.

Received: 7 May 2024 Accepted: 2 December 2024
Published online: 18 December 2024

References

1. Radoshevich L, Cossart P. *Listeria monocytogenes*: towards a complete picture of its physiology and pathogenesis. Nat Rev Microbiol. 2018;16(1):32–46. https://doi.org/10.1038/nrmicro.2017.126.
2. Cory L, Chu C. ADXS-HPV: a therapeutic *Listeria* vaccination targeting cervical cancers expressing the HPV E7 antigen. Hum Vaccin Immunother. 2014;10(11):3190–5. https://doi.org/10.4161/hv.34378.
3. Wood LM, Paterson Y. Attenuated *Listeria monocytogenes*: a powerful and versatile vector for the future of tumor immunotherapy. Front Cell Infect Microbiol. 2014;4:51. https://doi.org/10.3389/fcimb.2014.00051.
4. Portnoy DA, Auerbuch V, Glomski IJ. The cell biology of *Listeria monocytogenes* infection: the intersection of bacterial pathogenesis and cell-mediated immunity. J Cell Biol. 2002;158(3):409–14. https://doi.org/10.1083/jcb.200205009.
5. Tanaka A, Sakaguchi S. Regulatory T cells in cancer immunotherapy. Cell Res. 2017;27(1):109–18. https://doi.org/10.1038/cr.2016.151.
6. Shin JI, Ha SJ. Regulatory T cells-an important target for cancer immunotherapy. Nat Rev Clin Oncol. 2014;11(6):307. https://doi.org/10.1038/nrclinonc.2013.208-c1.
7. Chen Z, Ozbun L, Chong N, et al. Episomal expression of truncated listeriolysin O in LmddA-LLO-E7 vaccine enhances antitumor efficacy by preferentially inducing expansions of CD4+FoxP3- and CD8+ T cells. Cancer Immunol Res. 2014;2(9):911–22. https://doi.org/10.1158/2326-6066.CIR-13-0197.
8. Liang ZZ, Sherrid AM, Wallecha A, et al. *Listeria monocytogenes*: a promising vehicle for neonatal vaccination. Hum Vaccin Immunother. 2014;10(4):1036–46. https://doi.org/10.4161/hv.27999.
9. Flickinger JC Jr, Rodeck U, Snook AE. *Listeria monocytogenes* as a vector for cancer immunotherapy: Current understanding and progress. Vaccines (Basel). 2018;6(3):48. https://doi.org/10.3390/vaccines6030048.
10. Oladejo M, Paterson Y, Wood LM. Clinical experience and recent advances in the development of *Listeria*-based tumor immunotherapies. Front Immunol. 2021;12: 642316. https://doi.org/10.3389/fimmu.2021.642316.
11. Xu G, Feng D, Yao Y, et al. *Listeria*-based hepatocellular carcinoma vaccine facilitates anti-PD-1 therapy by regulating macrophage polarization. Oncogene. 2019;39:1429–44. https://doi.org/10.1038/s41388-019-1072-3.
12. Vitiello M, Evangelista M, Di Lascio N, et al. Antitumoral effects of attenuated *Listeria monocytogenes* in a genetically engineered mouse model of melanoma. Oncogene. 2019;38(19):3756–62. https://doi.org/10.1038/s41388-019-0681-1.
13. Jia YY, Tan WJ, Duan FF, et al. A genetically modified attenuated *Listeria* vaccine expressing HPV16 E7 kill tumor cells in direct and antigen-specific manner. Front Cell Infect Microbiol. 2017;7:279. https://doi.org/10.3389/fcimb.2017.00279.
14. Yang Y, Hou J, Lin Z, et al. Attenuated *Listeria monocytogenes* as a cancer vaccine vector for the delivery of CD24, a biomarker for hepatic cancer stem cells. Cell Mol Immunol. 2014;11(2):184–96. https://doi.org/10.1038/cmi.2013.64.
15. Shahabi V, Reyes-Reyes M, Wallecha A, et al. Development of a *Listeria monocytogenes* based vaccine against prostate cancer. Cancer Immunol Immunother. 2008;57(9):1301–13. https://doi.org/10.1007/s00262-008-0463-z.
16. Bruhn KW, Craft N, Miller JF. *Listeria* as a vaccine vector. Microbes Infect. 2007;9(10):1226–35. https://doi.org/10.1016/j.micinf.2007.05.010.
17. Gunn GR, Zubair A, Peters C, et al. Two *Listeria monocytogenes* vaccine vectors that express different molecular forms of human papilloma virus-16 (HPV-16) E7 induce qualitatively different T cell immunity that correlates with their ability to induce regression of established tumors immortalized by HPV-16. J Immunol. 2001;167(11):6471–9. https://doi.org/10.4049/jimmunol.167.11.6471.
18. Starks H, Bruhn KW, Shen H, et al. *Listeria monocytogenes* as a vaccine vector: Virulence attenuation or existing antivector immunity does not diminish therapeutic efficacy. J Immunol. 2004;173(1):420–7. https://doi.org/10.4049/jimmunol.173.1.420.
19. Olino K, Wada S, Edil BH, et al. Tumor-associated antigen expressing *Listeria monocytogenes* induces effective primary and memory T-cell responses against hepatic colorectal cancer metastases. Ann Surg Oncol. 2012;19(Suppl 3):S597-607. https://doi.org/10.1245/s10434-011-2037-0.
20. Brockstedt DG, Giedlin MA, Leong ML, et al. *Listeria*-based cancer vaccines that segregate immunogenicity from toxicity. Proc Natl Acad Sci U S A. 2004;101(38):13832–7. https://doi.org/10.1073/pnas.0406035101.
21. Li Z, Zhao X, Higgins DE, et al. Conditional lethality yields a new vaccine strain of *Listeria monocytogenes* for the induction of cell-mediated immunity. Infect Immun. 2005;73(8):5065–73. https://doi.org/10.1128/IAI.73.8.5065-5073.2005.
22. Shahabi V, Seavey MM, Maciag PC, et al. Development of a live and highly attenuated *Listeria monocytogenes*-based vaccine for the treatment of Her2/neu-overexpressing cancers in human. Cancer Gene Ther. 2011;18(1):53–62. https://doi.org/10.1038/cgt.2010.48.
23. Wallecha A, Maciag PC, Rivera S, et al. Construction and characterization of an attenuated *Listeria monocytogenes* strain for clinical use in cancer immunotherapy. Clin Vaccine Immunol. 2009;16(1):96–103. https://doi.org/10.1128/CVI.00274-08.

24. Saxena M, van der Burg SH, Melief CJM, et al. Therapeutic cancer vaccines. Nat Rev Cancer. 2021;21(6):360–78. https://doi.org/10.1038/s41568-021-00346-0.
25. Wood LM, Pan ZK, Shahabi V, et al. *Listeria*-derived ACTA is an effective adjuvant for primary and metastatic tumor immunotherapy. Cancer Immunol Immunother. 2010;59(7):1049–58. https://doi.org/10.1007/s00262-010-0830-4.
26. Cutts FT, Franceschi S, Goldie S, et al. Human papillomavirus and HPV vaccines: a review. Bull World Health Organ. 2007;85(9):719–26. https://doi.org/10.2471/blt.06.038414.
27. Sewell DA, Shahabi V, Gunn GR, et al. Recombinant *Listeria* vaccines containing PEST sequences are potent immune adjuvants for the tumor-associated antigen human papillomavirus-16 E7. Cancer Res. 2004;64(24):8821–5. https://doi.org/10.1158/0008-5472.CAN-04-1958.
28. Peng X, Treml J, Paterson Y. Adjuvant properties of listeriolysin O protein in a DNA vaccination strategy. Cancer Immunol Immunother. 2007;56(6):797–806. https://doi.org/10.1007/s00262-006-0240-9.
29. Kohda C, Kawamura I, Baba H, et al. Dissociated linkage of cytokine-inducing activity and cytotoxicity to different domains of listeriolysin O from *Listeria monocytogenes*. Infect Immun. 2002;70(3):1334–41. https://doi.org/10.1128/IAI.70.3.1334-1341.2002.
30. Wallecha A, Carroll KD, Maciag PC, et al. Multiple effector mechanisms induced by recombinant *Listeria monocytogenes* anticancer immunotherapeutics. Adv Appl Microbiol. 2009;66:1–27. https://doi.org/10.1016/S0065-2164(08)00801-0.
31. Bray F, Ferlay J, Soerjomataram I, et al. Global cancer statistics 2018: GLOBOCAN estimates of incidence and mortality worldwide for 36 cancers in 185 countries. CA Cancer J Clin. 2018;68(6):394–424. https://doi.org/10.3322/caac.21492.
32. Siegel RL, Miller KD, Jemal A. Cancer statistics, 2019. CA Cancer J Clin. 2019;69(1):7–34. https://doi.org/10.3322/caac.21551.
33. Ferris DG. Vaccines for preventing HPV-related anogenital infection and neoplasia. J Am Osteopath Assoc. 2006;106:S9-13.
34. Forman D, de Martel C, Lacey CJ, et al. Global burden of human papillomavirus and related diseases. Vaccine. 2012;30(Suppl 5):F12-23. https://doi.org/10.1016/j.vaccine.2012.07.055.
35. Jabbar SF, Park S, Schweizer J, et al. Cervical cancers require the continuous expression of the human papillomavirus type 16 E7 oncoprotein even in the presence of the viral e6 oncoprotein. Cancer Res. 2012;72(16):4008–16. https://doi.org/10.1158/0008-5472.CAN-11-3085.
36. Roden RBS, Stern PL. Opportunities and challenges for human papillomavirus vaccination in cancer. Nat Rev Cancer. 2018;18(4):240–54. https://doi.org/10.1038/nrc.2018.13.
37. Huang AY, Gulden PH, Woods AS, et al. The immunodominant major histocompatibility complex class I-restricted antigen of a murine colon tumor derives from an endogenous retroviral gene product. Proc Natl Acad Sci U S A. 1996;93(18):9730–5. https://doi.org/10.1073/pnas.93.18.9730.
38. Stringhini M, Spadafora I, Catalano M, et al. Cancer therapy in mice using a pure population of CD8(+) T cell specific to the AH1 tumor rejection antigen. Cancer Immunol Immunother. 2021;70(11):3183–97. https://doi.org/10.1007/s00262-021-02912-9.
39. Probst P, Kopp J, Oxenius A, et al. Sarcoma eradication by doxorubicin and targeted TNF Relies upon CD8(+) T-cell recognition of a retroviral antigen. Cancer Res. 2017;77(13):3644–54. https://doi.org/10.1158/0008-5472.CAN-16-2946.
40. Cheng C, Jiang L, Ma T, et al. Carboxyl-Terminal Residues N478 and V479 Required for the Cytolytic Activity of listeriolysin O Play a Critical Role in *Listeria monocytogenes* pathogenicity. Front Immunol. 2017;8:1439. https://doi.org/10.3389/fimmu.2017.01439.
41. Johansson J, Freitag NE. Regulation of *Listeria monocytogenes* virulence. Microbiol Spectr. 2019;7(4):GPP3–0064–2019. https://doi.org/10.1128/microbiolspec.GPP3-0064-2019
42. Vazquez-Boland JA, Wagner M, Scortti M. Why are some *Listeria monocytogenes* genotypes more likely to cause invasive (brain, placental) infection? mBio. 2020;11(6): e03126–20. https://doi.org/10.1128/mBio.03126-20
43. Li J, Sun Y, Garen A. Immunization and immunotherapy for cancers involving infection by a human papillomavirus in a mouse model. Proc Natl Acad Sci U S A. 2002;99(25):16232–6. https://doi.org/10.1073/pnas.192581299.
44. Scrimieri F, Askew D, Corn DJ, et al. Murine leukemia virus envelope gp70 is a shared biomarker for the high-sensitivity quantification of murine tumor burden. Oncoimmunology. 2013;2(11): e26889. https://doi.org/10.4161/onci.26889.
45. Ostroumov D, Fekete-Drimusz N, Saborowski M, et al. CD4 and CD8 T lymphocyte interplay in controlling tumor growth. Cell Mol Life Sci. 2018;75(4):689–713. https://doi.org/10.1007/s00018-017-2686-7.
46. Riazi Rad F, Ajdary S, Omranipour R, et al. Comparative analysis of CD4+ and CD8+ T cells in tumor tissues, lymph nodes and the peripheral blood from patients with breast cancer. Iran Biomed J. 2015;19(1):35–44. https://doi.org/10.6091/ibj.1289.2014.
47. Togashi Y, Shitara K, Nishikawa H. Regulatory T cells in cancer immunosuppression - implications for anticancer therapy. Nat Rev Clin Oncol. 2019;16(6):356–71. https://doi.org/10.1038/s41571-019-0175-7.
48. Galon J, Bruni D. Tumor Immunology and Tumor Evolution: Intertwined Histories. Immunity. 2020;52(1):55–81. https://doi.org/10.1016/j.immuni.2019.12.018.
49. Peng S, Tan M, Li YD, et al. PD-1 blockade synergizes with intratumoral vaccination of a therapeutic HPV protein vaccine and elicits regression of tumor in a preclinical model. Cancer Immunol Immunother. 2021;70(4):1049–62. https://doi.org/10.1007/s00262-020-02754-x.
50. Noubade R, Majri-Morrison S, Tarbell KV. Beyond cDC1: Emerging roles of DC crosstalk in cancer immunity. Front Immunol. 2019;10:1014. https://doi.org/10.3389/fimmu.2019.01014.
51. Wculek SK, Cueto FJ, Mujal AM, et al. Dendritic cells in cancer immunology and immunotherapy. Nat Rev Immunol. 2020;20(1):7–24. https://doi.org/10.3390/cancers16050981.
52. Borst J, Ahrends T, Babala N, et al. CD4(+) T cell help in cancer immunology and immunotherapy. Nat Rev Immunol. 2018;18(10):635–47. https://doi.org/10.1038/s41577-018-0044-0.
53. Bahrambeigi S, Shafiei-Irannejad V. Immune-mediated anti-tumor effects of metformin; targeting metabolic reprogramming of T cells as a new possible mechanism for anti-cancer effects of metformin. Biochem Pharmacol. 2020;174: 113787. https://doi.org/10.1016/j.bcp.2019.113787.
54. Bahrambeigi S, Molaparast M, Sohrabi F, et al. Targeting PPAR ligands as possible approaches for metabolic reprogramming of T cells in cancer immunotherapy. Immunol Lett. 2020;220:32–7. https://doi.org/10.1016/j.imlet.2020.01.006.
55. Chowdhury PS, Chamoto K, Kumar A, et al. PPAR-induced fatty acid oxidation in T cells increases the number of tumor-reactive CD8(+) T cells and facilitates Anti-PD-1 therapy. Cancer Immunol Res. 2018;6(11):1375–87. https://doi.org/10.1158/2326-6066.CIR-18-0095.
56. Wen T, Barham W, Li Y, et al. NKG7 is a T-cell-intrinsic therapeutic target for improving antitumor cytotoxicity and cancer immunotherapy. Cancer Immunol Res. 2022;10(2):162–81. https://doi.org/10.1158/2326-6066.CIR-21-0539.
57. Ye J, Ma C, Hsueh EC, et al. TLR8 signaling enhances tumor immunity by preventing tumor-induced T-cell senescence. EMBO Mol Med. 2014;6(10):1294–311. https://doi.org/10.15252/emmm.201403918
58. Pan ZK, Ikonomidis G, Lazenby A, et al. A recombinant *Listeria monocytogenes* vaccine expressing a model tumour antigen protects mice against lethal tumour cell challenge and causes regression of established tumours. Nat Med. 1995;1(5):471–7. https://doi.org/10.1038/nm0595-471.
59. Bruhn KW, Craft N, Nguyen BD, et al. Characterization of anti-self CD8 T-cell responses stimulated by recombinant *Listeria monocytogenes* expressing the melanoma antigen TRP-2. Vaccine. 2005;23(33):4263–72. https://doi.org/10.1016/j.vaccine.2005.02.018.
60. D'Orazio SEF. Innate and adaptive immune responses during *Listeria monocytogenes* infection. Microbiol Spectr. 2019;7(3):GPP3–0065–2019. https://doi.org/10.1128/microbiolspec.GPP3-0065-2019
61. Tangney M, Gahan CG. *Listeria monocytogenes* as a vector for anti-cancer therapies. Curr Gene Ther. 2010;10(1):46–55. https://doi.org/10.2174/156652310790945539.
62. Basu P, Mehta A, Jain M, et al. A randomized phase 2 study of ADXS11-001 *Listeria monocytogenes*-listeriolysin O immunotherapy with or without cisplatin in treatment of advanced cervical cancer. Int J Gynecol Cancer. 2018;28(4):764–72. https://doi.org/10.1097/IGC.0000000000001235.
63. Freitag NE, Rong L, Portnoy DA. Regulation of the prfA transcriptional activator of *Listeria monocytogenes*: multiple promoter elements contribute to intracellular growth and cell-to-cell spread. Infect Immun. 1993;61(6):2537–44. https://doi.org/10.1128/iai.61.6.2537-2544.1993.

64. Jones S, Portnoy DA. Characterization of *Listeria monocytogenes* pathogenesis in a strain expressing perfringolysin o in place of listeriolysin O. Infect Immun. 1994;62(12):5608–13. https://doi.org/10.1128/iai.62.12.5608-5613.1994.
65. Moors MA, Levitt B, Youngman P, et al. Expression of listeriolysin O and ACTA by intracellular and extracellular *Listeria monocytogenes*. Infect Immun. 1999;67(1):131–9. https://doi.org/10.1128/IAI.67.1.131-139.1999.
66. Portnoy DA, Jacks PS, Hinrichs DJ. Role of hemolysin for the intracellular growth of *Listeria monocytogenes*. J Exp Med. 1988;167(4):1459–71. https://doi.org/10.1084/jem.167.4.1459.
67. Chen C, Nguyen BN, Mitchell G, et al. The listeriolysin O PEST-like sequence Co-opts AP-2-mediated endocytosis to prevent plasma membrane damage during *Listeria* infection. Cell Host Microbe. 2018;23(6):786–95 e5. https://doi.org/10.1016/j.chom.2018.05.006
68. Verch T, Pan ZK, Paterson Y. *Listeria monocytogenes*-based antibiotic resistance gene-free antigen delivery system applicable to other bacterial vectors and DNA vaccines. Infect Immun. 2004;72(11):6418–25. https://doi.org/10.1128/IAI.72.11.6418-6425.2004.
69. Melief CJ, van Hall T, Arens R, et al. Therapeutic cancer vaccines. J Clin Invest. 2015;125(9):3401–12. https://doi.org/10.1038/s41568-021-00346-0.
70. Deng W, Lira V, Hudson TE, et al. Recombinant *Listeria* promotes tumor rejection by CD8(+) T cell-dependent remodeling of the tumor microenvironment. Proc Natl Acad Sci U S A. 2018;115(32):8179–84. https://doi.org/10.1073/pnas.1801910115.
71. Wallecha A, Wood L, Pan ZK, et al. *Listeria monocytogenes*-derived listeriolysin O has pathogen-associated molecular pattern-like properties independent of its hemolytic ability. Clin Vaccine Immunol. 2013;20(1):77–84.
72. Laidlaw BJ, Craft JE, Kaech SM. The multifaceted role of CD4(+) T cells in CD8(+) T cell memory. Nat Rev Immunol. 2016;16(2):102–11. https://doi.org/10.1128/CVI.00488-12.
73. Harari A, Graciotti M, Bassani-Sternberg M, et al. Antitumour dendritic cell vaccination in a priming and boosting approach. Nat Rev Drug Discov. 2020;19(9):635–52. https://doi.org/10.1038/s41573-020-0074-8.
74. Zenewicz LA, Shen H. Innate and adaptive immune responses to *Listeria monocytogenes*: A short overview. Microbes Infect. 2007;9(10):1208–15. https://doi.org/10.1016/j.micinf.2007.05.008.
75. Brzoza KL, Rockel AB, Hiltbold EM. Cytoplasmic entry of *Listeria monocytogenes* enhances dendritic cell maturation and T cell differentiation and function. J Immunol. 2004;173(4):2641–51. https://doi.org/10.4049/jimmunol.173.4.2641.
76. Szatmari I, Rajnavolgyi E, Nagy L. Ppargamma, a lipid-activated transcription factor as a regulator of dendritic cell function. Ann N Y Acad Sci. 2006;1088:207–18. https://doi.org/10.1196/annals.1366.013.
77. Széles L, Töröcsik D, Nagy L. Ppargamma in immunity and inflammation: Cell types and diseases. Biochim Biophys Acta. 2007;1771(8):1014–30. https://doi.org/10.1016/j.bbalip.2007.02.005.
78. Angela M, Endo Y, Asou HK, et al. Fatty acid metabolic reprogramming via mtor-mediated inductions of PPARγ directs early activation of T cells. Nat Commun. 2016;7:13683. https://doi.org/10.1038/ncomms13683.
79. Ahmadian M, Suh JM, Hah N, et al. PPARγ signaling and metabolism: the good, the bad and the future. Nat Med. 2013;19(5):557–66. https://doi.org/10.1038/nm.3159.
80. Hernandez-Quiles M, Broekema MF, Kalkhoven E. PPARgamma in metabolism, immunity, and cancer: Unified and diverse mechanisms of action. Front Endocrinol (Lausanne). 2021;12: 624112. https://doi.org/10.3389/fendo.2021.624112.
81. DeNardo DG, Ruffell B. Macrophages as regulators of tumour immunity and immunotherapy. Nat Rev Immunol. 2019;19(6):369–82. https://doi.org/10.1038/s41577-019-0127-6.
82. Facciabene A, Motz GT, Coukos G. T-regulatory cells: key players in tumor immune escape and angiogenesis. Cancer Res. 2012;72(9):2162–71. https://doi.org/10.1158/0008-5472.CAN-11-3687.
83. Zhang S, Ke X, Zeng S, et al. Analysis of CD8+ treg cells in patients with ovarian cancer: A possible mechanism for immune impairment. Cell Mol Immunol. 2015;12(5):580–91. https://doi.org/10.1038/cmi.2015.57.
84. Hussain SF, Paterson Y. CD4+CD25+ regulatory T cells that secrete TGFbeta and IL-10 are preferentially induced by a vaccine vector. J Immunother. 2004;27(5):339–46. https://doi.org/10.1097/00002371-200409000-00002.
85. Paluskievicz CM, Cao X, Abdi R, et al. T regulatory cells and priming the suppressive tumor microenvironment. Front Immunol. 2019;10:2453. https://doi.org/10.3389/fimmu.2019.02453.
86. Cinier J, Hubert M, Besson L, et al. Recruitment and expansion of tregs cells in the tumor environment-how to target them? Cancers (Basel). 2021;13(8):1850. https://doi.org/10.3390/cancers13081850.
87. Lin KY, Guarnieri FG, Staveley-O'Carroll KF, et al. Treatment of established tumors with a novel vaccine that enhances major histocompatibility class II presentation of tumor antigen. Cancer Res. 1996;56(1):21–6.
88. Duodu S, Mehmeti I, Holst-Jensen A, et al. Improved sample preparation for real-time PCR detection of *Listeria monocytogenes* in hot-smoked salmon using filtering and immunomagnetic separation techniques. Food Anal Methods. 2009;2(1):23–9. https://doi.org/10.1007/s12161-008-9043-2.
89. Pagliuso A, Tham TN, Allemand E, et al. An RNA-binding protein secreted by a bacterial pathogen modulates RIG-I signaling. Cell Host Microbe. 2019;26(6):823–35. https://doi.org/10.1016/j.chom.2019.10.004.
90. David DJ, Pagliuso A, Radoshevich L, et al. Lmo1656 is a secreted virulence factor of *Listeria monocytogenes* that interacts with the sorting nexin 6-BAR complex. J Biol Chem. 2018;293(24):9265–76. https://doi.org/10.1074/jbc.RA117.000365.
91. Xayarath B, Alonzo F 3rd, Freitag NE. Identification of a peptide-pheromone that enhances *Listeria monocytogenes* escape from host cell vacuoles. Plos Pathog. 2015;11(3): e1004707. https://doi.org/10.1371/journal.ppat.1004707.
92. Reniere ML, Whiteley AT, Portnoy DA. An *in vivo* selection identifies *Listeria monocytogenes* genes required to sense the intracellular environment and activate virulence factor expression. Plos Pathog. 2016;12(7): e1005741. https://doi.org/10.1371/journal.ppat.1005741.
93. LADS: A Powerful Vaccine Platform for Cancer Immunotherapy and Prevention. RNA sequencing data. https://www.ncbi.nlm.nih.gov/bioproject/PRJNA1190894/ (2024)
94. Bubert A, Kuhn M, Goebel W, et al. Structural and functional properties of the p60 proteins from different *Listeria* species. J Bacteriol. 1992;174(24):8166–71. https://doi.org/10.1128/jb.174.24.8166-8171.1992.

Publisher's Note